CFD simulation of gas dispersion at hydrogen bunkering station

Suwon Choi & Byongug Jeong

Published online: 04 Oct 2023.

Submit your article to this journal ☒

Article views: 96

View related articles ☒

View Crossmark data ☒

Taylor & Francis
Taylor & Francis Group

CFD simulation of gas dispersion at hydrogen bunkering station

Suwon Choi[a,b,c] and Byongug Jeong [ID][a,c]

[a]Department of Naval Architecture, Ocean and Marine Engineering, University of Strathclyde, Glasgow, UK; [b]Navalship Integreated/Structure Design Team, Hanwha Ocean, Geo-je, Korea; [c]Europe-Korea Marine and Ocean Engineers Association (EKMOA), Southampton, UK

ABSTRACT

This research is to simulate hydrogen leakage at bunker station with various wind directions and velocities using Computational Fluid Dynamics (CFD) model to understand hydrogen dispersion behaviour and provide general guidelines to establish risk prevent measures and mitigations at early design phase. This case study examines hydrogen plume behavior in various wind conditions, focusing on horizontal and vertical dispersion as well as mean travel distance over time. Regardless of wind direction, hydrogen disperses in alignment with the wind. As time progresses post-leakage, the plume elongates in the wind's longitudinal direction and contracts vertically, maintaining a consistent shape. Wind direction and the direction of hydrogen release notably influence dispersion patterns. When the wind aligns vertically with the release point, hydrogen plume distance increases with higher wind speeds. Conversely, when wind opposes the release direction, plume length tends to decrease at high speeds. Intriguingly, the maximum distance of 27.85 m occurs when wind and leak directions are orthogonal at 180°. For wind speeds up to 5 m/s, all wind directions show a similar increase in plume distance. However, at 7 m/s, scenarios with horizontal, perpendicular wind directions exhibit a distinct change. Analyzing hydrogen dispersion aids in establishing safety criteria and risk mitigation distances for hydrogen leakages in bunker stations during the early design phase.

Introduction

Background

The International Maritime Organization (IMO) has recently implemented regulations on air pollutant emissions and is actively discussing market-based measures for decarbonisation in the international shipping sector. Based on the Fourth IMO GHG Study 2020 released by the IMO, it was reported that international shipping was responsible for emitting 740 million tonnes of CO_2 in 2018, which accounted for 2.89% of global CO_2 emissions (C. IMO, 2020). During the 72nd MEPC meeting in April 2018 (IMO, 2018), the Initial Strategic was adopted to reduce greenhouse gas emissions. The goal is to achieve a reduction of over 50% in international shipping emissions by 2050 compared to 2008 levels, with specific targets and timelines for carbon zero (Figure 1).

It is essential to apply all available innovative technologies within the ship and shipping industry to achieve the goals for the GHG reduction set by IMO in the shipping sector. The heavy fuel oil currently used for combustion engines in most commercial ships results in significant CO_2 emissions and natural gas, which is used for a substitute of heavy fuel oil to reduce CO_2 emissions by only 5% to 30% compared to traditional fuels (Bouman et al., 2017). In addition, as a secondary measure to reduce carbon emissions, various methods are being implemented, including the LNG-powered ships, the adoption of low-sulphur oil, and the installation of exhaust gas treatment devices. However, since these methods still rely on fossil fuels, they have limitations in complying with the increasingly stringent CO_2 regulations. Therefore, it is obviously challenging to meet the long-term emission reduction targets using conventional fossil fuels, but it is essential to adopt environmentally friendly alternative fuels and develop innovative technologies for this fuels. Hydrogen would be in the limelight as an alternative of fossil fuel among the clean resources under consideration of its environmental effect. When it use as fuel it has zero carbon emission and based on how it is generated, the emission of CO_2 can be lowered to achieve the target (Atilhan et al., 2021).

Characteristics of hydrogen as an alternative marine fuel

Hydrogen is abundantly present in nature and can be found in various mixtures. It is the lightest element and also the most reactive. In the industry, hydrogen is classified into two categories based on the generation
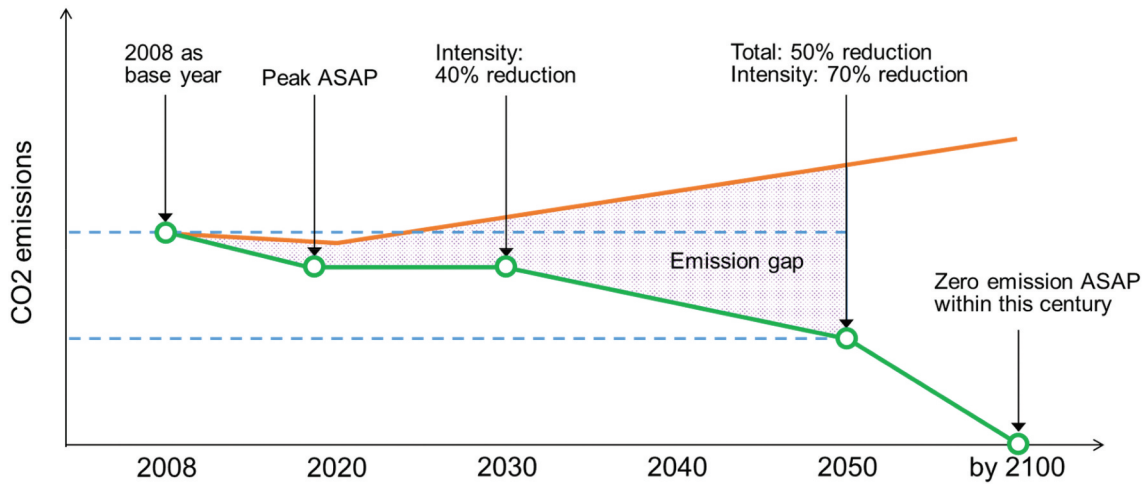
Figure 1. IMO initial strategy on reduction of greenhouse gas emission.
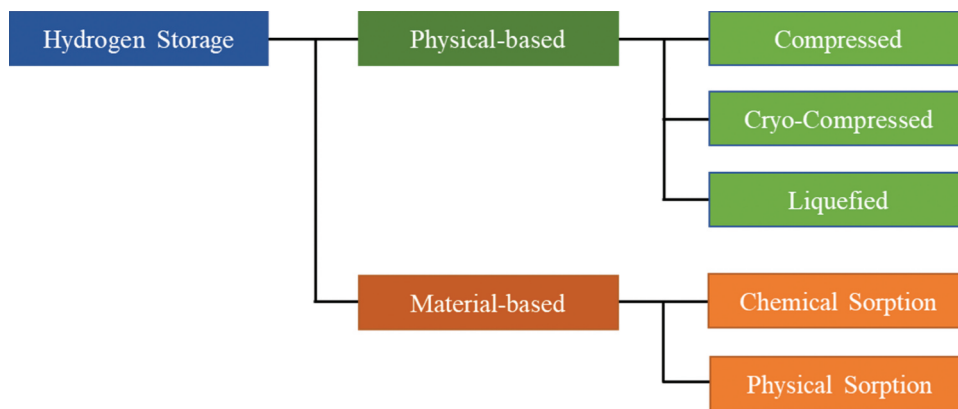

Figure 2. Storage methods for hydrogen.

method: grey hydrogen and green hydrogen. Grey hydrogen is produced with carbon emissions and includes hydrogen obtained as a by product of the oil refining process and hydrogen generated through carbon formation. The most common method is to extract hydrogen and carbon dioxide from methane obtained through a steam reforming process of natural gas (Hyde et al., 2019). This method is the least expensive way to produce hydrogen, but it results in significant CO2 emissions, which greatly diminishes the primary advantage of using hydrogen as a fuel. Consequently, a crucial measure to address this issue is the implementation of carbon capture and storage (CCS) technology. On the other hand, green hydrogen refers to hydrogen produced without carbon emissions, which includes hydrogen generated from renewable energy sources or nuclear power. The most common method involves obtaining hydrogen through the electrolysis process, which splits water into hydrogen and oxygen (Hyde et al., 2019). This method is currently the subject of extensive research as a sustainable approach, particularly when performed using electricity generated from renewable resources. Notably, electrolysis conducted with renewable energy sources produces no carbon emissions, making it a highly sought-after technique. To utilise hydrogen as a fuel in

ships, understanding hydrogen storage is of paramount importance. Currently, there is active development of technologies for converting compressed hydrogen, liquefied hydrogen, LOHC (Liquid Organic Hydrogen Carrier), or ammonia.

Following table shows chemical properties of hydrogen comparing to the MGO and LNG which are most widely used as marine fuel (G.S. CENTER, 2021).

Hydrogen has the highest energy per mass with 120.2 MJ/kg amongst fuels as shown in the Table 1, and it is approximately 2.8 times for MGO and 2.5 times for LNG. For this reason, hydrogen would be considered as more energy efficient fuel and reduce fuel consumption significantly. However, the energy density of hydrogen is lower than MGO and LNG, which means a larger space to contain hydrogen is necessary to carry an equivalent amount of energy.

Fire risk and safety

Flammable ranges typically pertain to vapours and are characterized as the concentration span within which a combustible substance can trigger a fire or explosion upon the presence of an ignition source.
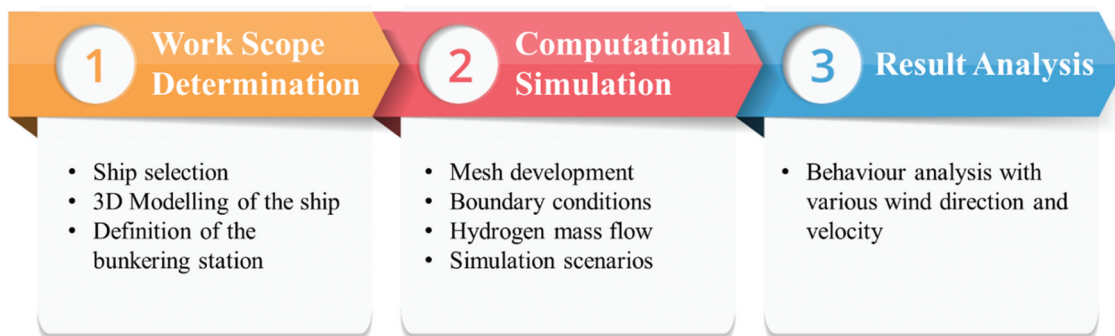
1 **Work Scope Determination**
- Ship selection
- 3D Modelling of the ship
- Definition of the bunkering station

2 **Computational Simulation**
- Mesh development
- Boundary conditions
- Hydrogen mass flow
- Simulation scenarios

3 **Result Analysis**
- Behaviour analysis with various wind direction and velocity

Figure 3. Methodology for the study.

Plan View

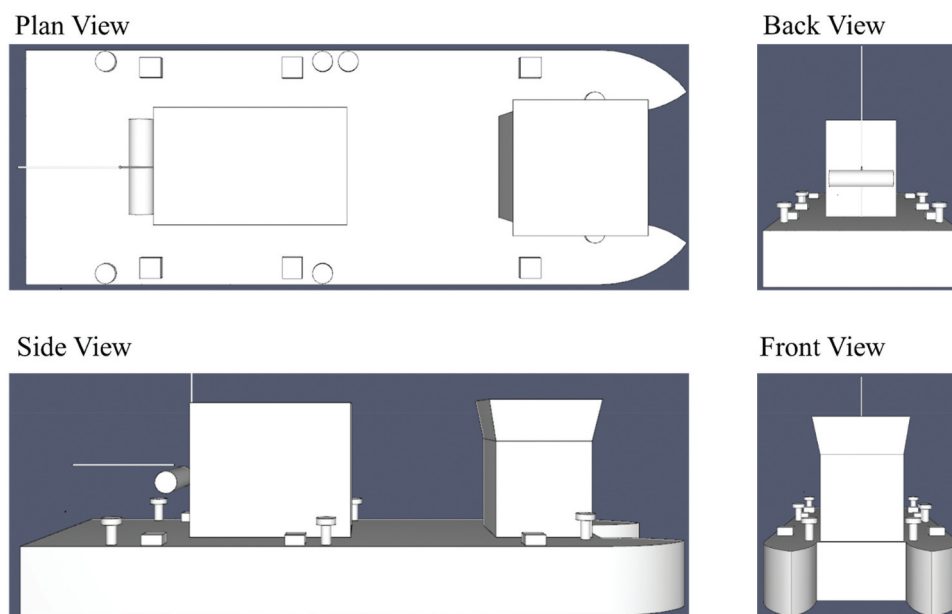Back View

Side View

Front View

Figure 4. 3D model result of the vessel.

The concentration is generally expressed as percent fuel by volume with lower flammable limit (LFL) and upper flammable limit (UFL). Ignition energy is necessary energy to ignite a mixture vapour within a flammable limit and the values in the Table 1 are minimum energy for ignition. Also, deflagration index indicates that pressure rate in case of explosion. Therefore, the flammable limits, ignition energy, and deflagration index can be used as indicators of the ease with which a fire or explosion can occur and the extent to which it can propagate. Hydrogen has higher danger in case an explosion with wider flammability limits, lower ignition energy, and higher deflagration index from Table 1.

When hydrogen burns alone, it produces only water vapour without smoke. The flame temperature reaches 2,130 ℃, but it emits significantly less radiant heat compared to hydrocarbon combustion. As a result, it becomes difficult to detect the flame until direct

Table 1. Chemical properties for typical fuel types.

Property	Hydrogen	MGO	Methane (LNG)
Boiling Point (℃)	−253	180–360	−161
Density (kg/m3)	70.8	900	430
Lower Heating Value (MJ/kg)	120.2	42.7	48
Auto Ignition Temp (℃)	585	250	537
Flashpoint (℃)	-	>60	−188
Energy Density Liquid (MJ/L)	8.51	38.4	20.6
Compared Volume to MGO (H2 Gas at 700 bar)	4.51	1	1.86
Lower Flammability Limit (% vol. fraction)	4	0.7	5.3
Upper Flammability Limit (% vol. fraction)	75	5	17
Minimum Ignition Energy (mJ)	0.017	-	0.274
Deflagration index	550	100–150	30.4–86

Table 2. Characteristic of physical-based storage method.

| Storage method	Temperature (K)	Pressure (bar)	Advantages	Limitations	Applications
Compressed gas hydrogen	−40 ~ 27	150–800	Light-weight	Low energy density; up to 10% energy loss in the compression process	Small-scale storage; mobile applications such as hydrogen-powered vehicles
Cryo-compressed hydrogen	−240 ~ −196	150–350	High energy density	Require strict insulation	Medium to large-scale storage; transportation such as truck delivery and international hydrogen shipping
Liquefied hydrogen	−253 ~ −240	1–12.76	High energy density	Require strict insulation; up to 40% energy consumption in liquefaction processes	Medium to large-scale storage; transportation such as truck delivery and international hydrogen shipping

Table 3. Representative loss of containment scenarios.

Scenario	Truck to ro-ro ship	Ship to ro-ro ship	Ship to container ship
Hose leak	1.5×10^{-4}/h	7.3×10^{-5}/h	6.2×10^{-5}/h
Hose rupture	1.5×10^{-5}/h	7.3×10^{-6}/h	6.2×10^{-5}/h
Manifold leak	1×10^{-5}/m	5×10^{-6}/m	5×10^{-7}/h
Manifold rupture	2×10^{-6}/m	1×10^{-6}/m	1×10^{-7}/m
Tank rupture from ship striking	N/A	1.25×10^{-8}/h	1.25×10^{-8}/m
Hose rupture from ship striking	N/A	$0.006 \times f_0$*	$0.006 \times f_0$*

* f_0 equals $6.7 \cdot 10^{-11} \cdot T \cdot t \cdot N$, where T is the total number of ships per year on the transport route or in the harbour, t is the average duration of loading unloading per ship (in hours) and N is the number of transhipments per year.

Table 4. Principal dimension of the vessel.

Main principal dimensions			
Length overall (L_{OA})	:	18.50	m
Length between the perpendiculars (L_{BP})	:	18.00	m
Breadth (Moulded)	:	7.00	m
Depth (Moulded)	:	1.80	m
Draft	:	1.00	m

contact is made, increasing the risk of severe burns. Moreover, this characteristic of hydrogen combustion leads to poor visibility, allowing the fire to propagate unnoticed (HYSAFE, 2007). Most hazardous hydrogen incidents involve either buoyant or momentum-driven behaviour. In cases where high-pressure hydrogen is
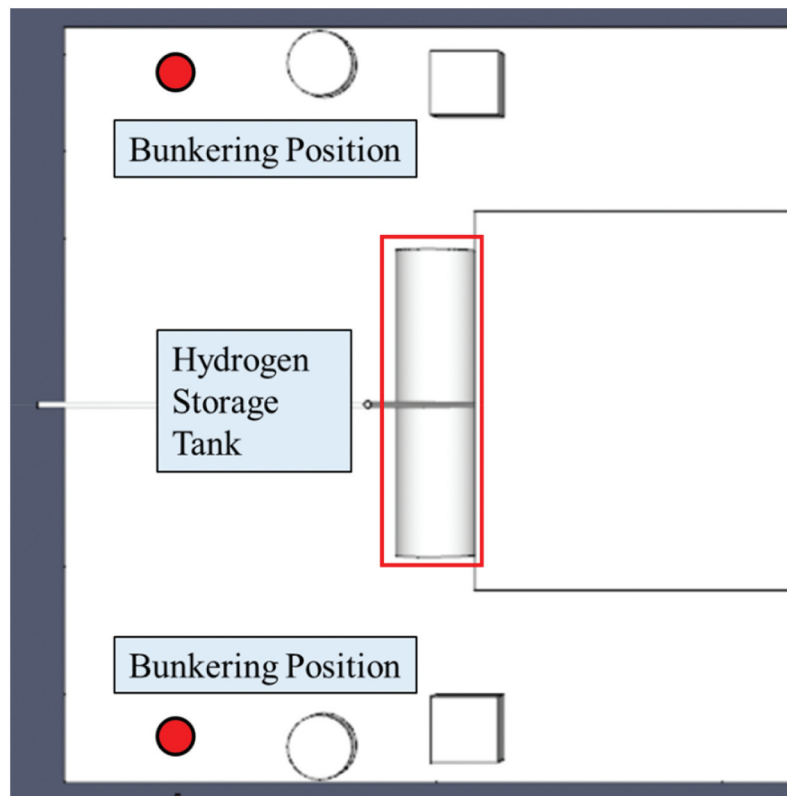
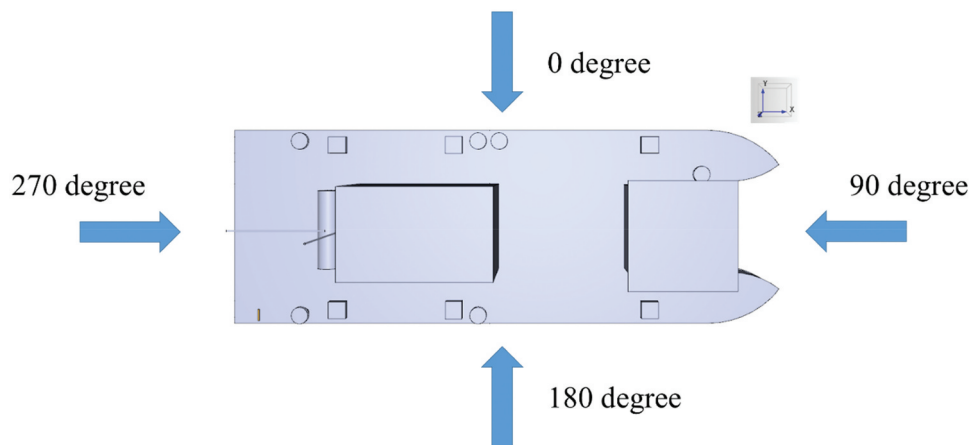**Figure 5.** Storage tank and bunkering position of the ship.

Figure 6. Wind direction.

Table 5. Bunkering duration for equivalent amounts of energy.

Recourse	Pressure (MPa)	Flow Rate (m³/hour)	Internal Hose Diameter (mm)	Bunkering Duration (hours/year)
LNG	0.022	400	150	250
Ammonia	9	400	150	495
Hydrogen Gas	70	5.65	25	86,605
	38	**122**	**50**	**6,236**

released near a storage tank due to an accident, a large fireball of several tens of meters can immediately form, and the presence of obstacles or the level of confinement significantly affects the flame's behaviour (Tretsiakova McNally, 0000).

Literature review

Hydrogen is the most abundant and lightest element on Earth; it is commonly present in a compounded state, bound to other elements. Hydrogen is a gaseous energy carrier which is carbon-free. These unique attributes have drawn significant attention within the shipping industry, appealing policymakers, researchers, and companies alike. Moreover, hydrogen's potential in shipping is experiencing a rapid surge, complementing its growing adoption in various transportation sectors, including automobiles (Inal et al., 2022). A fuel cell is a device that directly converts chemical energy into electricity through an electrochemical reaction between oxygen in the air and hydrogen or a hydrogen-containing fuel. For hydrogen fuel cell ship, hydrogen shall be provided by utilising hydrogen, LNG, methane, or ammonia as a resource to generate electricity through a fuel cell and uses this electricity to operate a motor for propulsion.

Table 6. Leakage scenarios in according to various wind conditions.

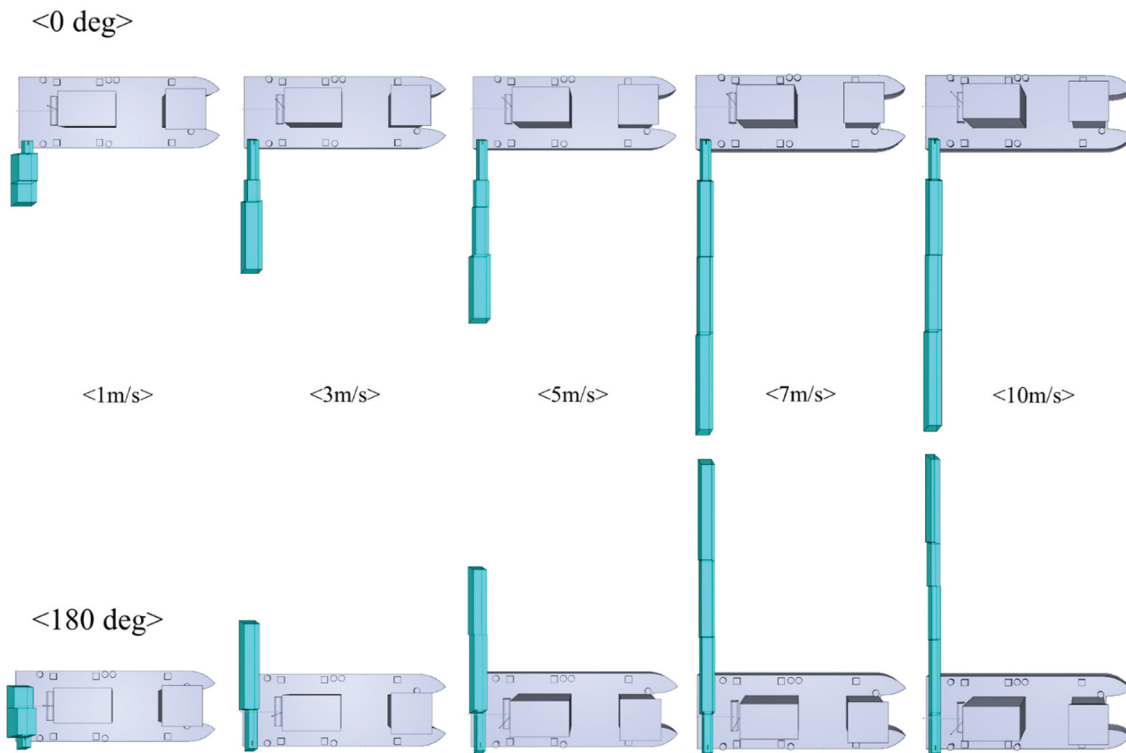| Scenario	Volume flow rate (m3/hour)	Wind Direction	Wind velocity (m/s)
1		0 degrees	1.00
2		(from port to starboard)	3.00
3			5.00
4			7.00
5			10.00
6		90 degrees	1.00
7		(from bow to stern)	3.00
8			5.00
9	122		7.00
10			10.00
11		180 degrees	1.00
12		(from starboard to port)	3.00
13			5.00
14			7.00
15			10.00
16		270 degrees	1.00
17		(from stern to bow)	3.00
18			5.00
19			7.00
20			10.00

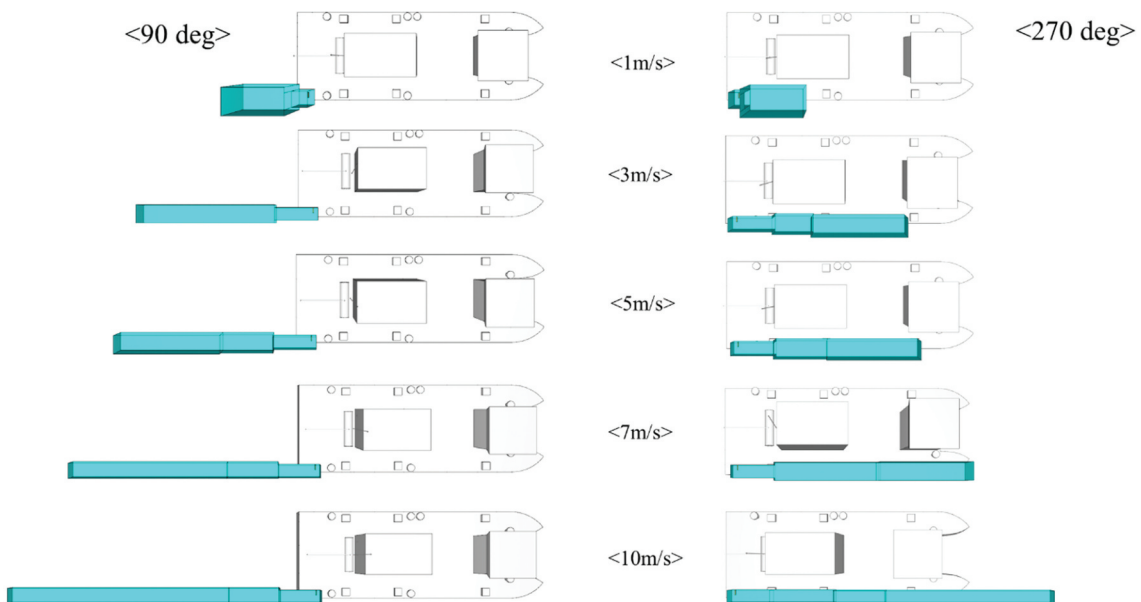**Figure 7.** Mesh configuration of wind direction of 0° and 180°.

Figure 8. Mesh configuration of wind direction of 90° and 270°.

Storage methods for hydrogen could be categorised into material-based and physical-based methods such as Figure 2 (Moradi & Groth, 2019).

A material-based storage method uses chemical absorption and physical adsorption to convert hydrogen gas to solid states. However, technical readiness level for this is low comparing to physical-based methods (Wang et al., 2021). On the other hands, physical-based method can be mainly categorised into three storage methods such as liquefied hydrogen, cryo-compressed hydrogen, and compressed gas hydrogen (Wang et al., 2021). The cryo-compressed hydrogen method was introduced to compensate high energy consumption of liquefied hydrogen storage (Durbin & Malardier-Jugroot, 2013). Table 2 shows characteristic of each storage method.

In theory, LOHC could be a one of solution for hydrogen-fuelled ships to zero carbon, but there are still too many uncertainties about the system.
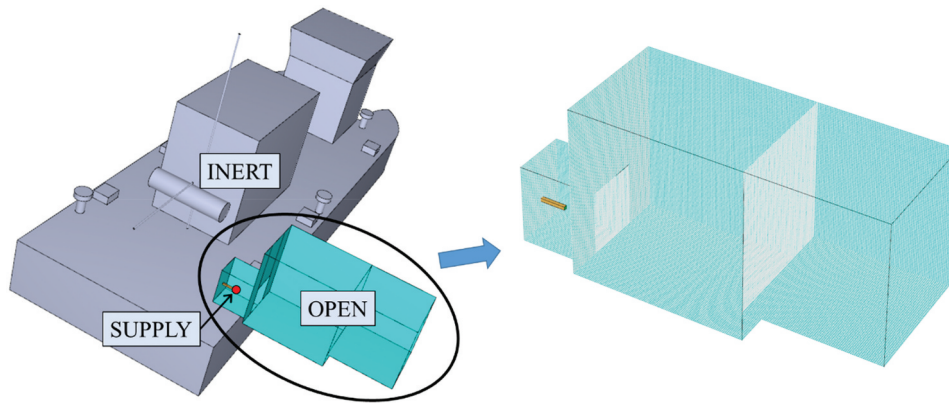
Figure 9. Definition of boundary conditions and detail of grid.

Table 7. Maximum travel distance and steady mean distance for each wind velocity at wind direction 0°.

Wind velocity (m/s)	Maximum horizontal distance (m)	Maximum vertical distance (m)	Mean distance at steady state (m)
1	4.44	2.54	3.23
3	11.15	1.86	4.67
5	16.22	1.58	6.47
7	23.79	1.22	12.50
10	22.68	1.18	14.21

Liquefied hydrogen is considered the most viable option for international shipping due to its highest volumetric energy density of the three storage modes. When using liquefied hydrogen, it is advantageous to configure it with a gas engine so that evaporation of liquefied hydrogen can be accelerated using engine heat (Hyde et al., 2019). However, the use of liquefied hydrogen storage is limited due to challenges associated with its low level of technological advancement, significant boil-off concerns, and demanding high insulation requirements (Ratnakar et al., 2021). Compressed hydrogen is a currently widely used option for various vehicle types. Storing fuel at a pressure of 700 bar offers high energy density. However, as the pressure increases, the fuel equipment becomes more complex, resulting in significant cost escalation. On the other hand, compressed hydrogen at 350 bar has a lower energy density. Nonetheless, refuelling technology at this pressure has been commercially available for an extended period and requires much smaller investment compared to liquid hydrogen or high compressed hydrogen equipment. As a result, larger vehicles like buses and trains typically employ 350 bar pressure hydrogen technology. Despite these advantages, compressed hydrogen is not suitable for large ships, except for regular short routes such as ferries, due to the low flow rate and substantial storage space requirements. Consequently, compressed hydrogen offers a short-term and appropriate solution for hydrogen-fuelled ships (Hyde et al.,

2019). For this reason, many ferries and ships operated in coastal waters around the world are built and operated using compressed hydrogen as fuel.

Hydrogen-fuelled ship and infrastructures for bunkering is not fully developed yet, and it is only been experienced in recent years of bunkering, even though LNG has been widely used as marine fuel for a decade with many experiences, and there are huge researches on risk during bunkering. Therefore, risk during LNG bunkering had been reviewed to recognise most risk scenario for hydrogen bunkering.

Ventikos, Podimatas, and Koimtzoglou (Ventikos et al., 2022) conducted a Quantitative Risk Assessment (QRA) for a case study on LNG bunkering at the Port of Piraeus. The study examined failure frequencies based on different scenarios, ship types, and LNG transfer methods. Table 3 indicates the result of the research and the hose leak is the most frequently occurred failure scenario at every case.

In addition to the Ventikos et al's study, Ahn, Kurt, and Turan (Ahn et al., 2022) revealed the influence of human factors on the stability of LNG bunkering systems. While the inclusion of an independent Emergency Stop Device (ESD) does not have a significant impact on overall system reliability, the additional supervisor at the workstation has been found to enhance the reliability of whole system. This outcome highlights the substantial role of humans in ensuring system reliability, rather than the influence of other components. Moreover, the study emphasises that the importance of human involvement becomes increasingly pronounced in complicated systems.

Swain, Filoso, and Swain (Swain et al., 2007) found that the leakage rate of the hydrogen plume with a concentration of 4% increased as the Mach number increased, and the difference between the calculated distance and the experimental result increased. Shu, Liang, Zheng, Lei, Cao, Dai, and Qian (Shu et al., 2021) were able to compare the experiment and the prediction model and obtained a result extending from the lowest axis but was close to the axis, confirming that it increased by enabling it. There was also an experiment to show increasing hydrogen release void or
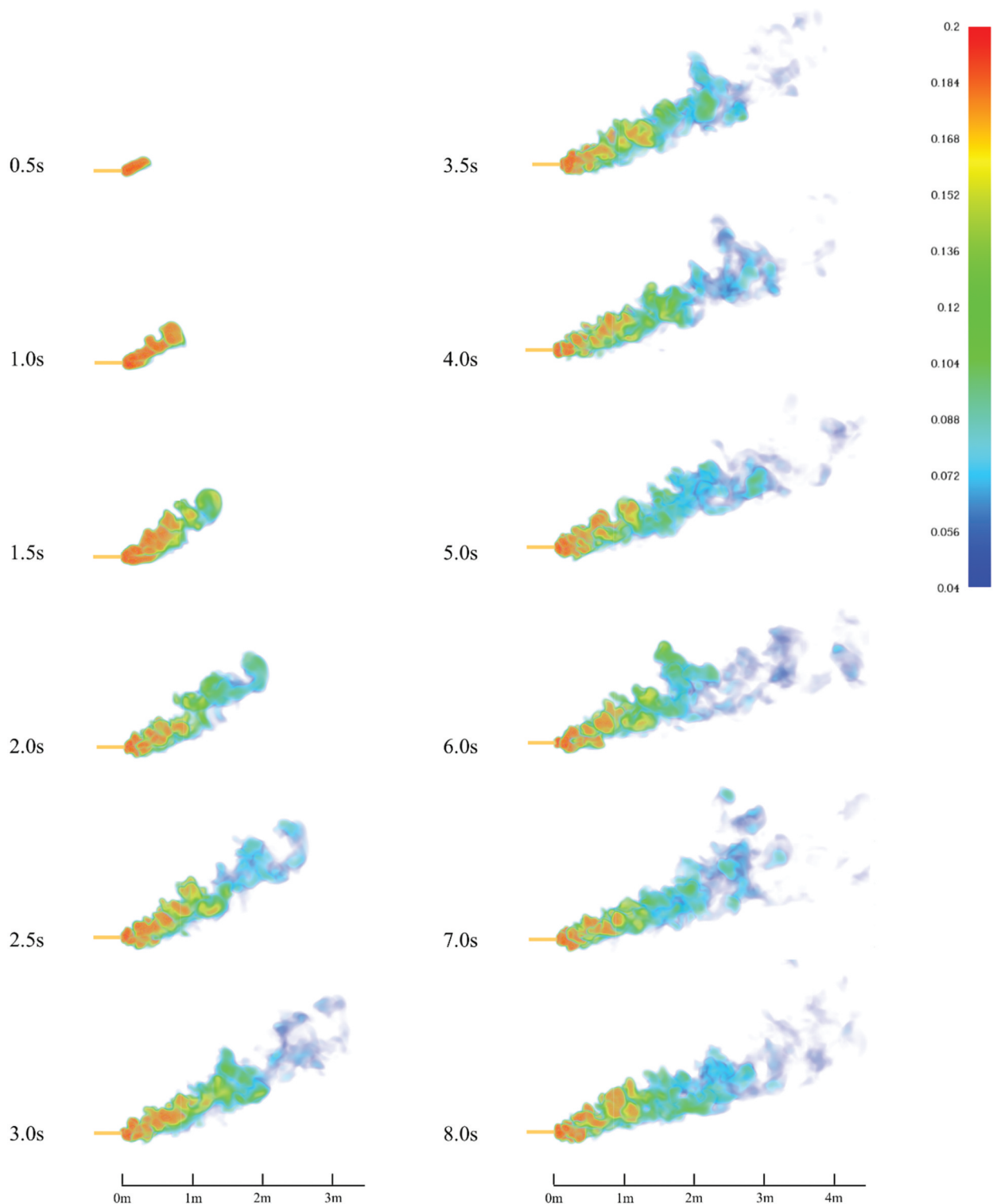
Figure 10. Hydrogen dispersion at 0° and wind velocity 1 m/s (S1).

decreasing gas release rate reduces buoyancy motion in the upward hydrogen jet (Brzezińska, 2021). The experiment by Witcofski and Chirivella (Witcofski & Chirivella, 1984) confirmed that hydrogen leaked near the ground mixes rapidly with air and becomes buoyant due to turbulence, phase shifts, and thermal instability. De Stefano, Rocourt, Sochet, and Daudey (De Stefano et al., 2019) revealed that the hydrogen dispersion is much more dependent on the flow rate than the location of the leak via experiments.

Regarding flow rate, Venetsanos, Baraldi, Adams, Heggem, and Wilkening (Venetsanos et al., 2008) proved via Computational Fluid Dynamics (CFD) that the pressure of my tank compression increases the stopping power. A paper confirmed how ship motion affects hydrogen leakage. Kim and Hwang (Kim & Hwang, 2023) examined the hydrogen concentration was affected by roll and pitch, and pitch had more influence than roll and they had same result through CFD (Kim & Hwang, 2022).
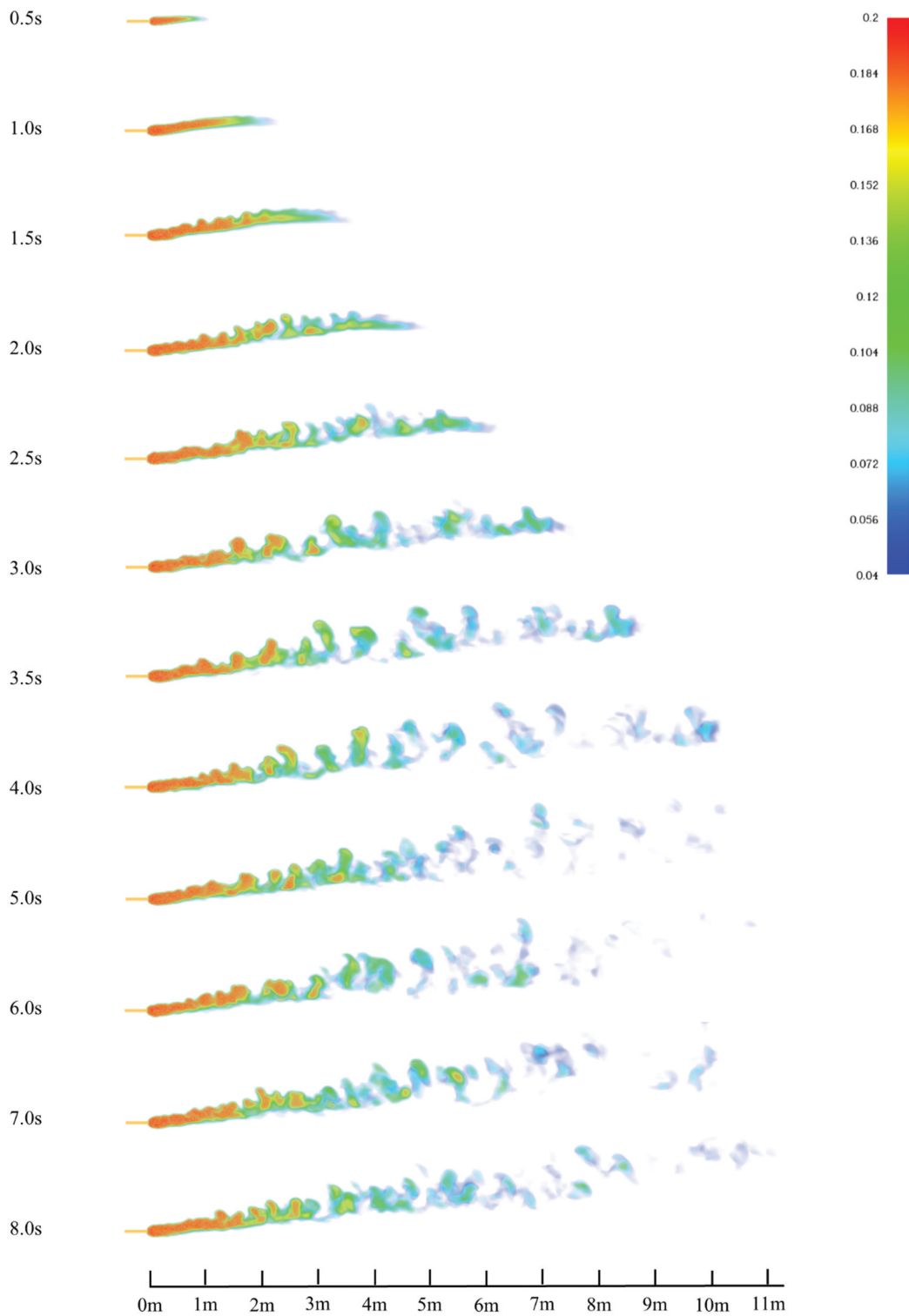
Figure 11. Hydrogen dispersion at 0° and wind velocity 3 m/s (S2).

There are many papers to study hydrogen dispersion after leakage through CFD recently. Middha, Hansen, and Storvik (Middha et al., 2009) carried out a study to validate similarity between CFD simulation and experimental results for hydrogen leakage of subsonic jet, and this study shows CFD simulation is reliable. This is well indicated in another paper issued by Prankul Middha (Middha et al., 2010). He simulated hydrogen leakage with three different nozzle sizes, 100 mm, 21 mm, and 1 mm. The 21 mm nozzle case was most well fit with experimental result, and the 100 mm with lower moment had lower predictions. Therefore, this paper revealed limitation of CFD simulation for large diameter nozzles. Furthermore, In addition, according to the CFD analysis performed by Goswami and Sun (Goswami & Sun, 2022), good agreement was achieved, with an average deviation of about 10%, even in the case of a high-speed hydrogen leak of 53 m/s. It is anticipated that CFD simulation is reliable with range of 100 mm nozzle size and 53 m/s leakage velocity. Liu, Zheng, Xu, Zhao, Bie, Chen, and Dryver (Liu et al.,
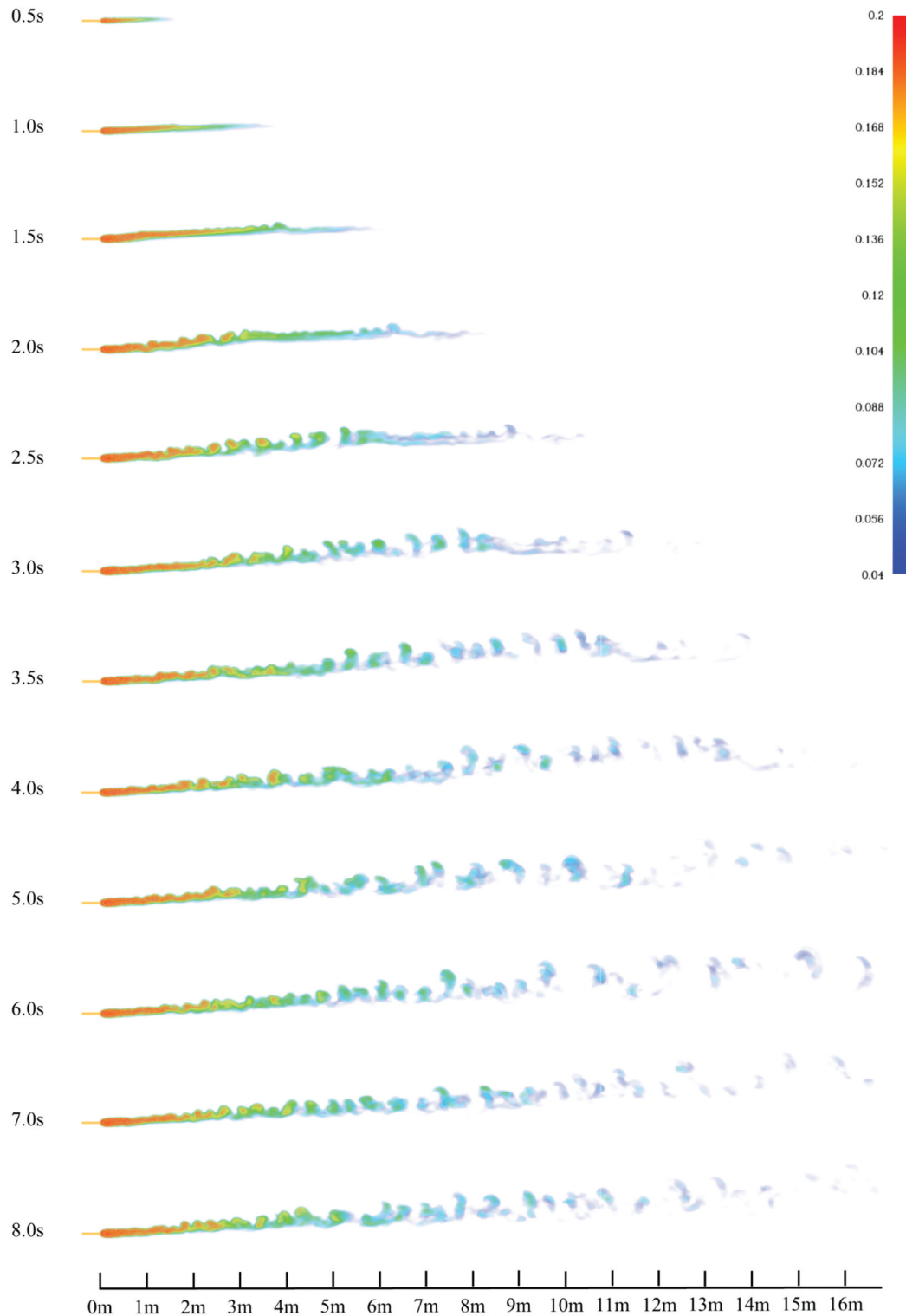
Figure 12. Hydrogen dispersion at 0° and wind velocity 5 m/s (S3).

2009) studied a dispersion characteristics of hydrogen by leakage from a compressed storage through numerical simulation. The simulation was conducted with a hole size of 0.5 mm to 5 mm on the storage tank and 2 mm with various wind velocity range under 40MPa. Also, the research performed by Qian, Li, Gao, and Jin (Qian et al., 2020) shows the simulation result from refuelling station in enclosed space. This research occurred that hydrogen behaviour in case leakages from 40MPa storage tank on the 10 mm dimeter hole with two different directions. In the two papers, simulations were conducted to analyse various leak directions, wind velocities, and leak sizes. However, the focus was solely on leaks resulting from tank damage. The research by Tofalos, Jeong, and Jang (Tofalos et al., 2020) indicates that the probability of tank damage is 9.459×10^{-4}, which is considerably lower than the probability of leakage through a bunkering hose. Choi, Hur, Kang, Lee and Lee (Choi et al., 2013), Huang,
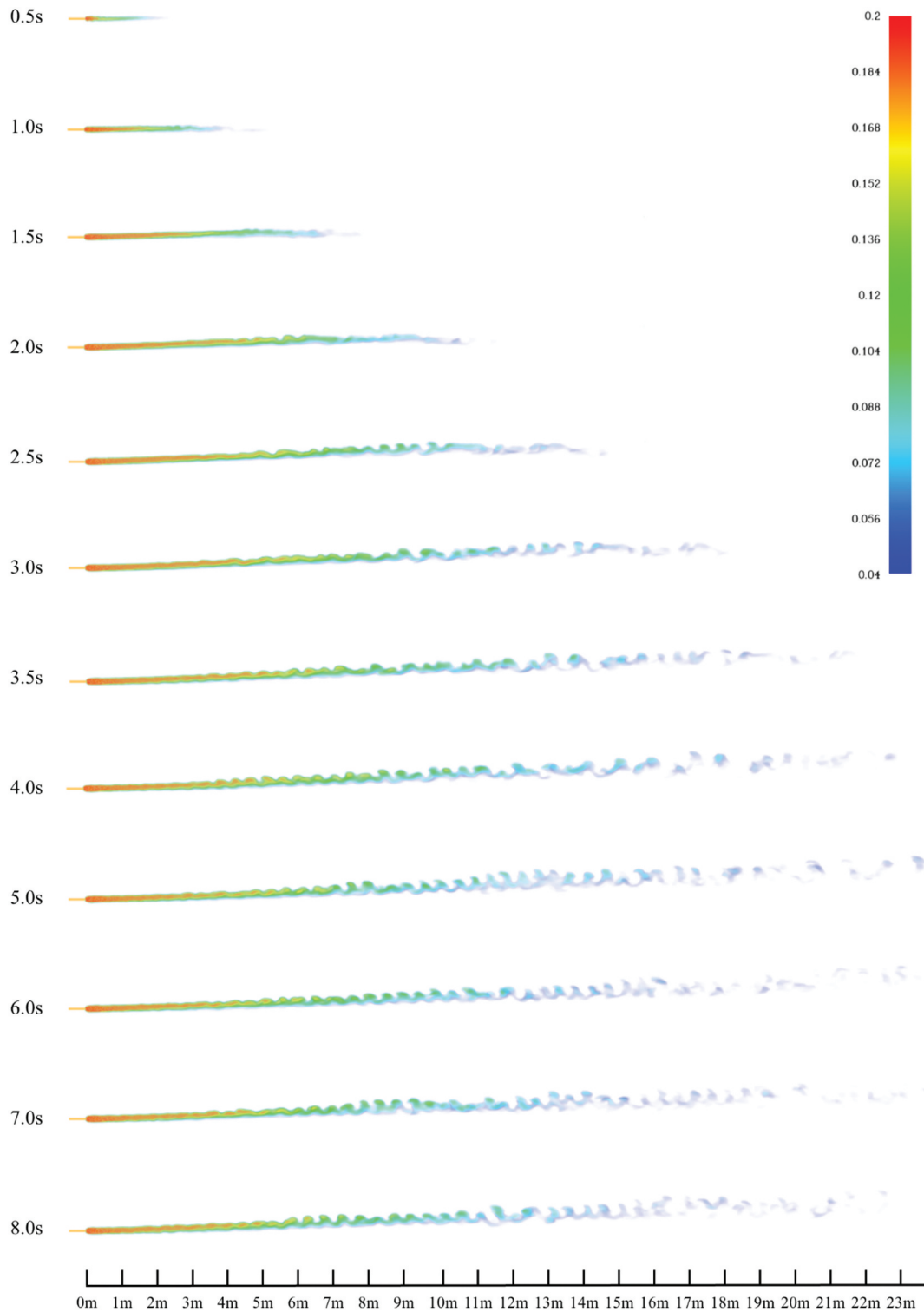
Figure 13. Hydrogen dispersion at 0° and wind velocity 7 m/s (S5).

Zhao, Ba, Christopher and Li (Huang et al., 2022) and Dadashzadeh, Ahmad, and Khan (Dadashzadeh et al., 2016) studied the relationship between hydrogen leakage behaviour and ventilation. The studies revealed significant changes in the combustible area based on air volume linked to hydrogen's rapid diffusion rate. Hydrogen accumulation at wall corners reduced ventilation effectiveness. Another paper demonstrated the behaviour of the hydrogen plume generated from the vent mast through CFD (Blaylock & Klebanoff, 2022). The

wind direction was set at 45 degrees below the horizontal direction on the vent mast, and the leakage speed at the vent mast was divided into 860 m/s and 10 m/s for the simulation. This study revealed that the dispersion of hydrogen is strongly influenced by the leak rate. Another study examines the impact of environmental factors on leakage (Mousavi & Parvini, 2016). It indicates that recent discharge rate is influenced by these factors, while humidity, temperature, and external pressure have minimal or negligible effects.
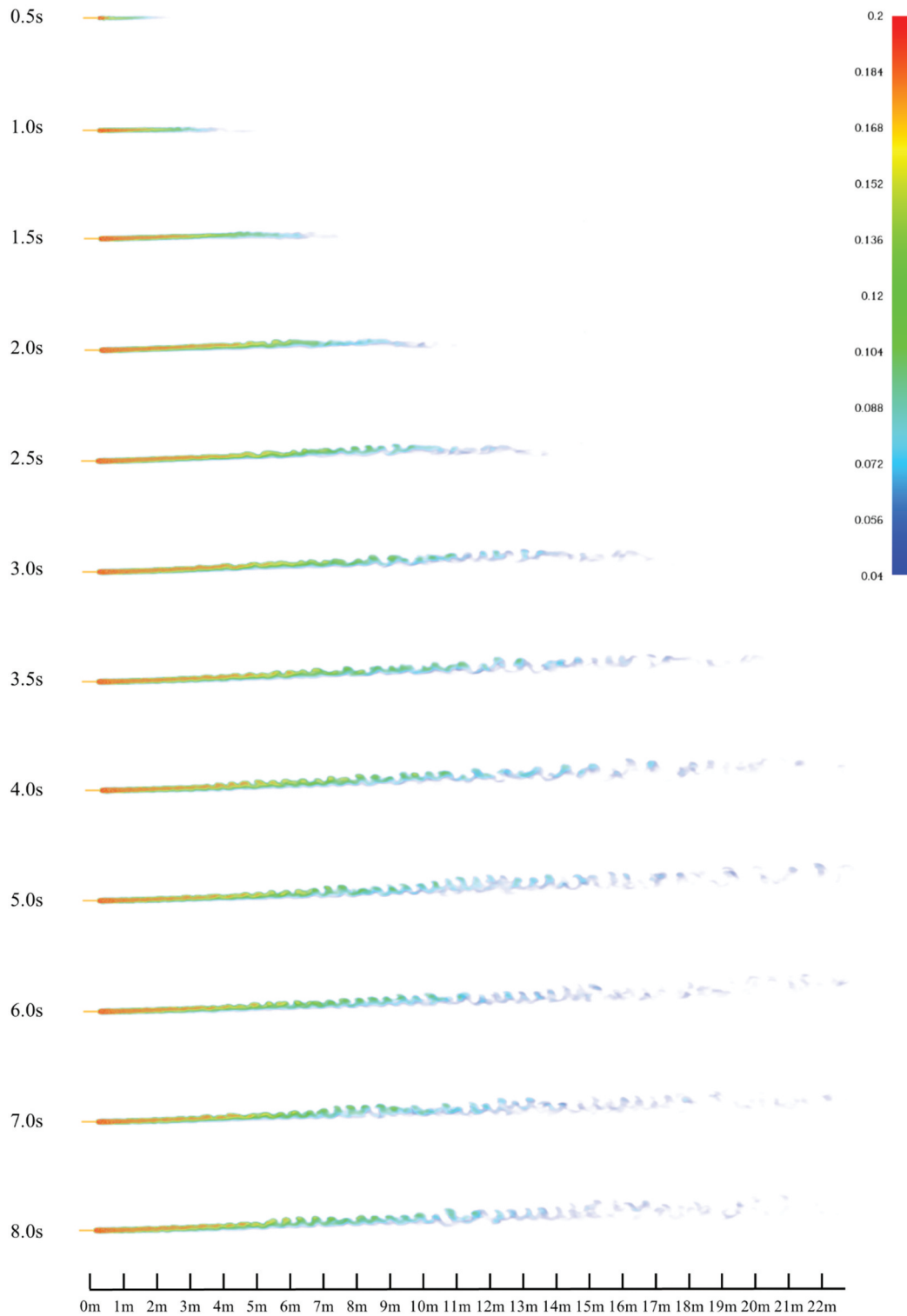
Figure 14. Hydrogen dispersion at 0° and wind velocity 10 m/s (S5).

Due to the safety issue, helium can be experimentally considered as a substitution of hydrogen as it simulate hydrogen dispersion (He et al., 2016). According to study by Xin, Duan, Jin, and Sun (Xin et al., 2023), helium dispersion grows rapidly immediately after ejection and then becomes relatively stable. In general, larger leak flow rates and larger nozzle diameters lead to higher helium concentrations. However, the effect of nozzle diameter is only apparent at large leak rates, and the diameter does not significantly affect the far-field concentration.

From the reviewed literatures, it was confirmed that the compressed hydrogen fuelled ships are suitable for short voyage ships. However, researches for a direct hydrogen leakage from a hose of a bunker station has not been conducted yet, even though the hose leak incident by human error is one of the most frequent leakage failure type. For this reason, the research idea is to investigate the potential risks and safety concerns associated with leakage at a bunker station of a vessel using compressed
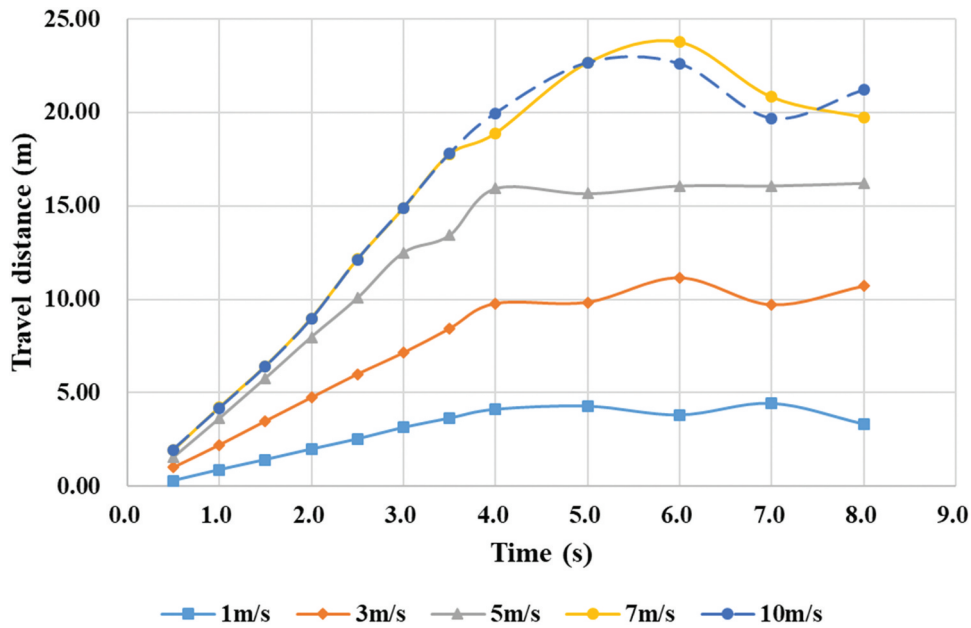
Figure 15. Maximum travel distance of hydrogen at wind direction 0°.

hydrogen. The aim of the study is to simulate the propagation distance of hydrogen leakage under various wind directions and velocities using 3D CFD in order to assess the potential impact on crew safety and the surrounding environment. The main objective of the study is to identify and mitigate the risks associated with hydrogen as a fuel for the shipping industry, particularly at the bunker station.

The research objectives include:

- To create a 3D CFD model of a bunker station configuration for a hydrogen-fuelled vessel.
- To determine potential scenarios for hydrogen leakage at the bunker station.
- To simulate the propagation of hydrogen in the bunker station using 3D CFD.
- To propose potential safety measures to enhance the safety of the bunker station and reduce the risk of hydrogen leakage.

By achieving these objectives, the study will contribute to the advancement of sustainable fuel options for the maritime industry. The research is important in addressing the safety concerns associated with hydrogen as a marine fuel, particularly at the bunker station, and promoting the safe and sustainable use of hydrogen in the shipping industry.

Case study

In this study, two reliable software, SOLIDWORKS by Dassault Systèmes and SolidWorks Corporation and PyroSim by Thunderhead Engineering, are used for a development of 3D vessel and a simulation CFD for leakage of hydrogen gas, relatively.

As outlined below, the project methodology primarily consists of three steps aimed at observing the behaviour of hydrogen gas leakage during bunkering.

The first step is Scope Determination During this initial step, the specific research scope for the project was established. A study plan was devised to comprehensively understand the potential phenomena associated with hydrogen leaks. To achieve this, the following factors must be taken into account:

- Ship dimensions and lines
- Definition of the bunkering station
- Assumptions to be applied

Having defined the research scope, the second step involved developing a numerical model for simulating hydrogen leaks using CFD. Careful attention must be given to the numerical modelling process, as it significantly impacts the accuracy of the analysis results. Furthermore, the simulation should be given sufficient time to reach a steady state. The following considerations should be taken into account during this step:

- Mesh resolution
- Boundary conditions
- Hydrogen mass flow
- Definition of leakage scenarios

In the final step, the results obtained from the gas leak simulation, specifically the behaviour of compressed hydrogen gas leaking from the ship's bunkering station, were compared and analysed in relation to the wind direction and intensity. Figure 3 shows overall methodoloy for this research.
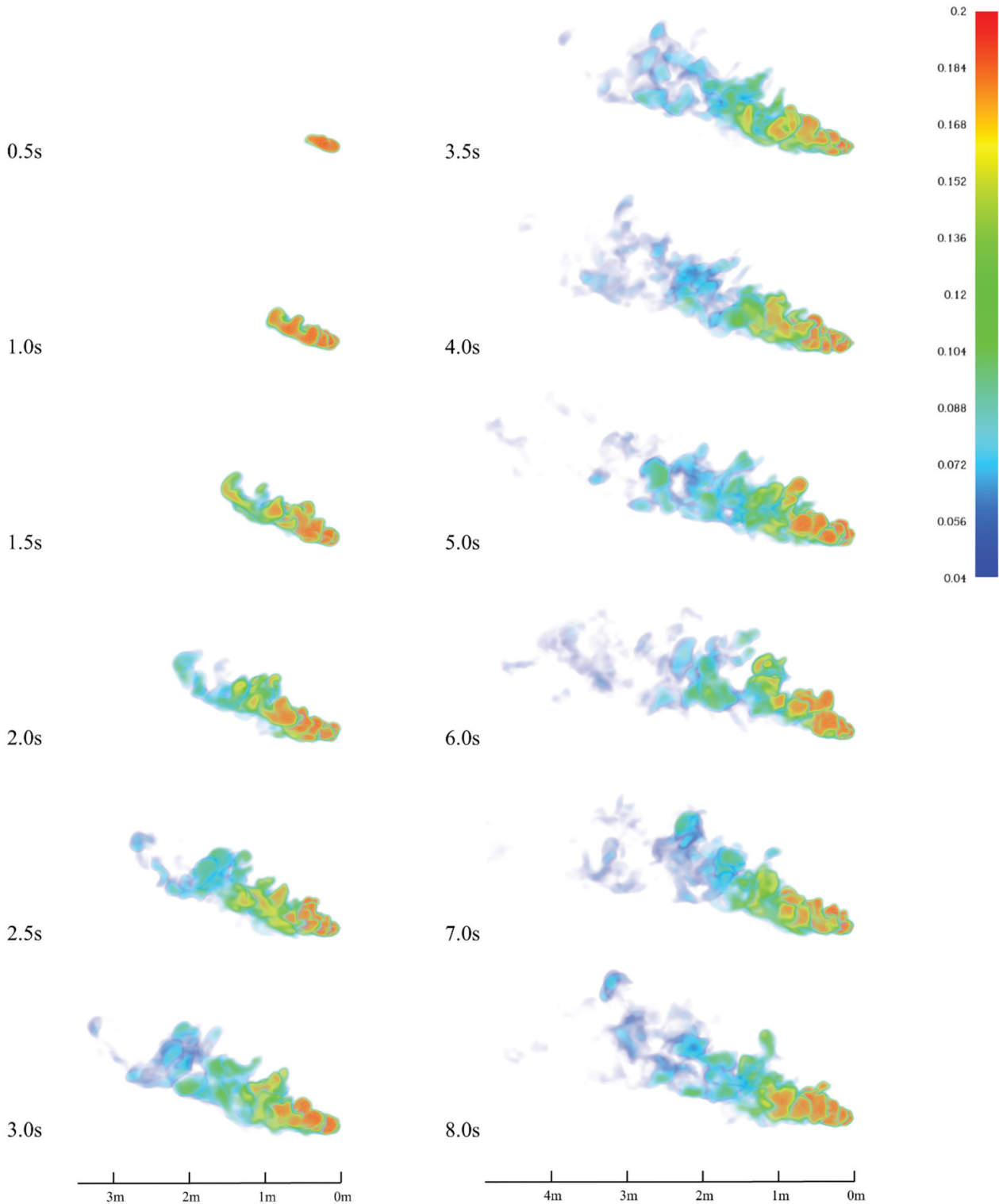
Figure 16. Hydrogen dispersion at 90° and wind velocity 1 m/s (S6).

Work scope determination

Ship selection

The benchmarked ship of this project, named the Cheonghang Ship, is a vessel that handles marine floating debris operated by the Korea Marine Environment Corporation. It is a 20-ton ammonia-fueled electric propulsion vessel. It is designed to operate for a maximum of 8 hours at a top speed of 10 knots. As the primary power source, it is equipped with two 25 kW fuel cells and two 75 kWh batteries, capable of generating a total of 150 kWh of electricity per hour. The propulsion of the target ship relies on two 50 kW motors, and the ship's operational plan is designed to consume 40 kW per motor, equivalent to a maximum of 80 kWh per hour. The principal dimension of the vessel is shown in Table 4.

Although this ship is not a vessel that directly uses compressed hydrogen, it is suitable as a demonstration ship for this study because it is composed of a very similar appearance and system to a hydrogen-fuelled
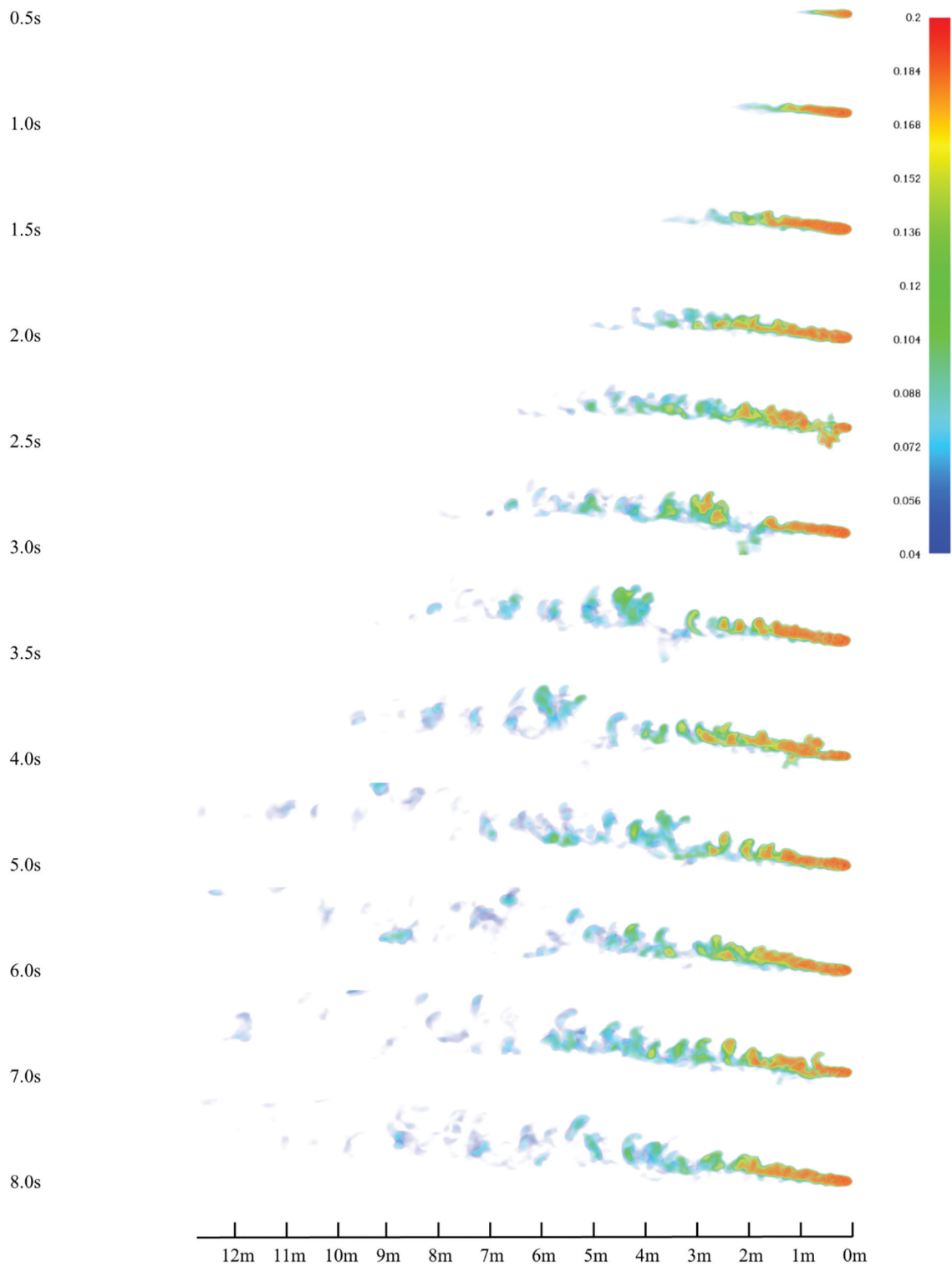
Figure 17. Hydrogen dispersion at 90° and wind velocity 3 m/s (S7).

ship except for the hydrogen reforming part. Also, the shape and arrangement of equipment and structures on the main deck of a ship can vary based on factors such as size, type of ship, and the specific layout of the bunker station. When hydrogen leakage occurs and is dispersed on the main deck, the shape of the deck itself can directly influence the behaviour of the gas plume. However, this study focuses on a specific small ship, which may not fully represent the diverse situations and vessel types encountered in practice.

3D modelling of the ship

The demonstration vessel was simplified and developed based on 2D drawings and principal dimensions. It features a catamaran design instead of a traditional monohull, which allows for better handling of marine debris. As a result, the width of the vessel is significantly large and the main deck area is spacious. The forward section of the vessel accommodates a bridge, while a hydrogen gas
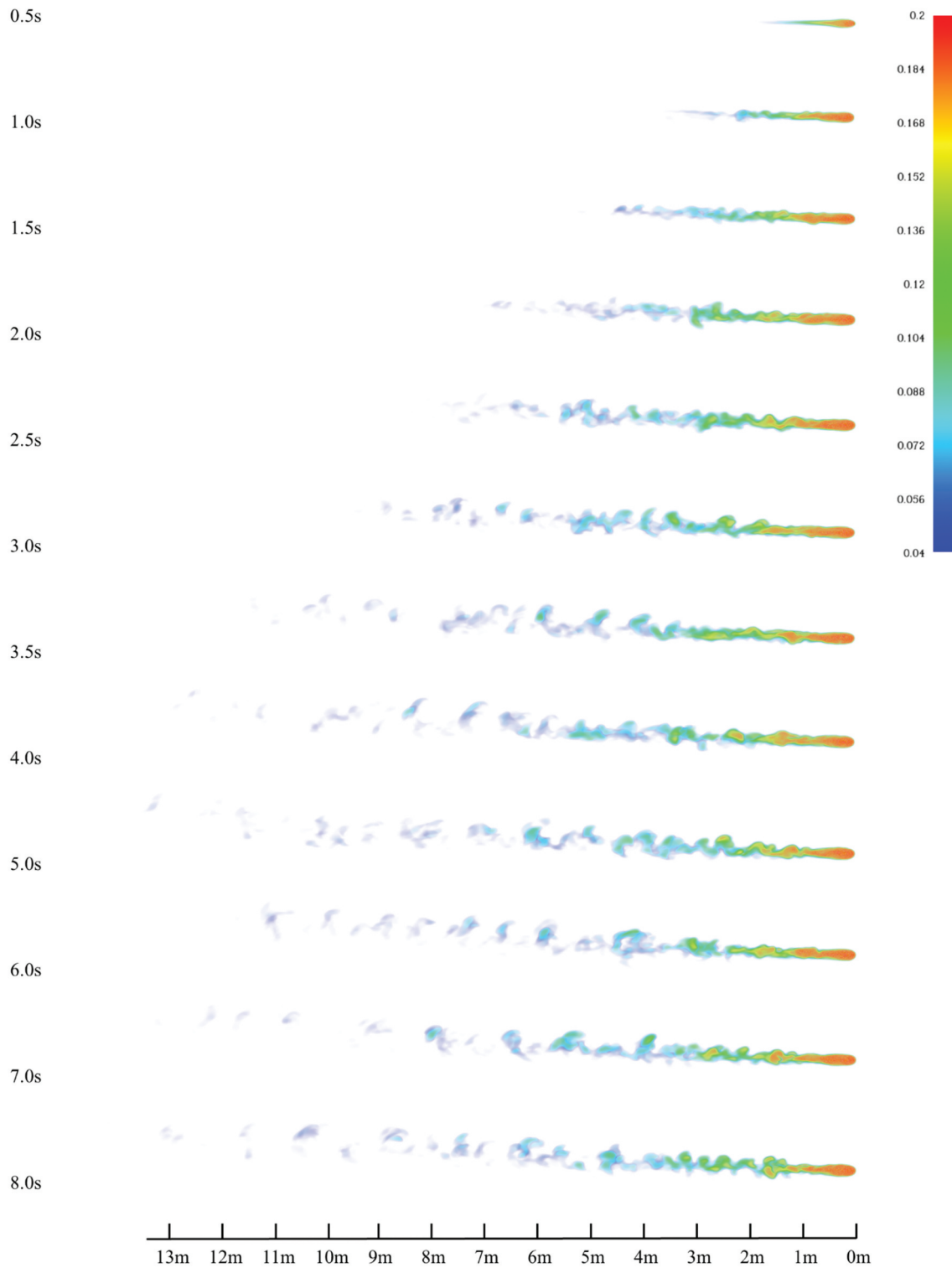
Figure 18. Hydrogen dispersion at 90° and wind velocity 5 m/s (S8).

storage tank and bunkering facility is provided on the stern areas. Additionally, waste disposal facilities are located in the ship's centre. For the purpose of analysing the impact of hydrogen leakage on the main deck, box modelling was employed, simplifying the bridge, and waste disposal facilities. Figure 4 shows 4 views of 3D model.

Bunkering station

Based on the design result of the demonstrated ship, hydrogen storage tank is also located on the aft main deck. Even though any rule and regulation for hydrogen bunker station has not been established yet, but LNG bunker station shall be arranged under consideration of below by ABS (ABS).
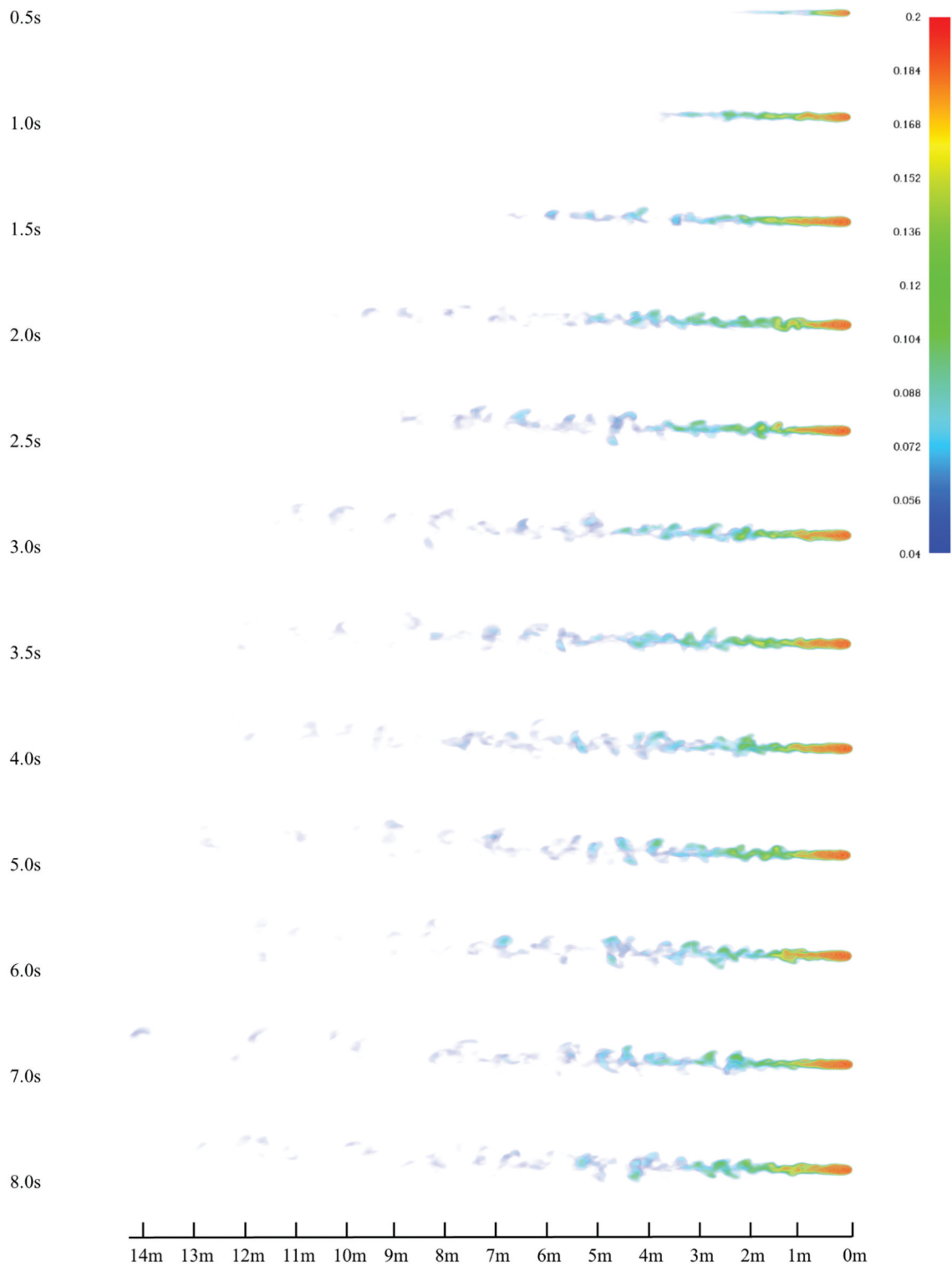
Figure 19. Hydrogen dispersion at 90° and wind velocity 7 m/s (S9).

(i) The bunkering station is to be located on the open deck to provide sufficient so that sufficient natural ventilation is provided.

(ii) The bunker manifold and connections are to be visible from the bunkering control station and cargo control station or bridge, as applicable. Remote video arrangements may be accepted where direct line of sight from the aforementioned locations is not possible.

Therefore, with applying a similar logic to determine bunkering station, it is assumed most part of main deck at each side of ship to minimize any risk might occur during operation. Figure 5 shows approximate position
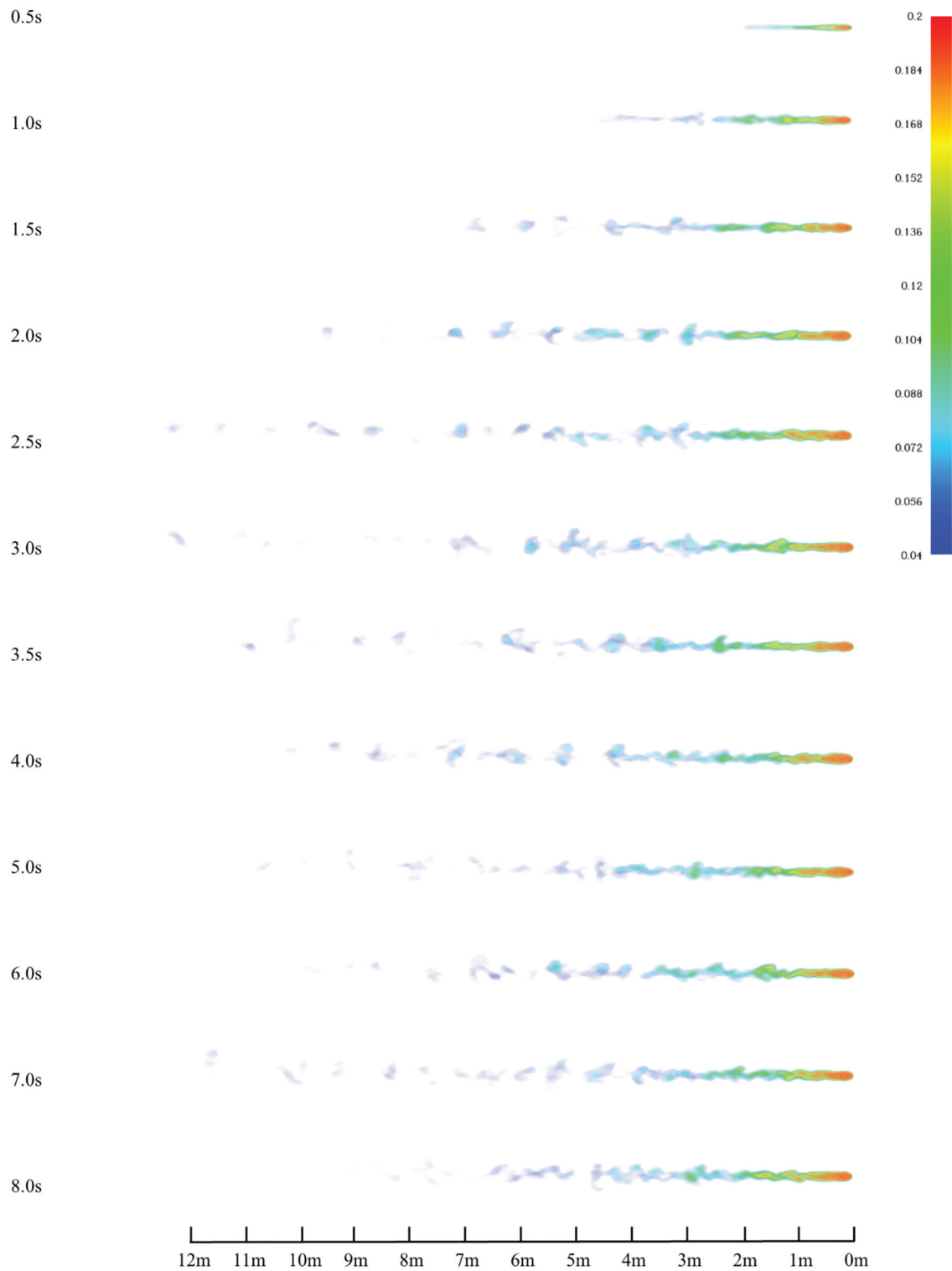
Figure 20. Hydrogen dispersion at 90° and wind velocity 10 m/s (S10).

of bunker stations and storage tank. The ship is exactly symmetric, so the simulation is only carried out for the starboard bunker position.

Computational simulation

Gas dispersion analysis simulations involve solving equations for mass conservation, momentum conservation, and species transport equation. PyroSim, a software tool, is capable of simulating the diffusion of a compressible gas in turbulent fluid flow field in three dimensions by employing a mathematical model based on the aforementioned equations.

The mass conservation equation

The equation of mass conservation could be written by;-

Figure 21. Maximum travel distance of hydrogen at wind direction 90°.

Table 8. Maximum travel distance and steady mean distance for each wind velocity at wind direction 90°.

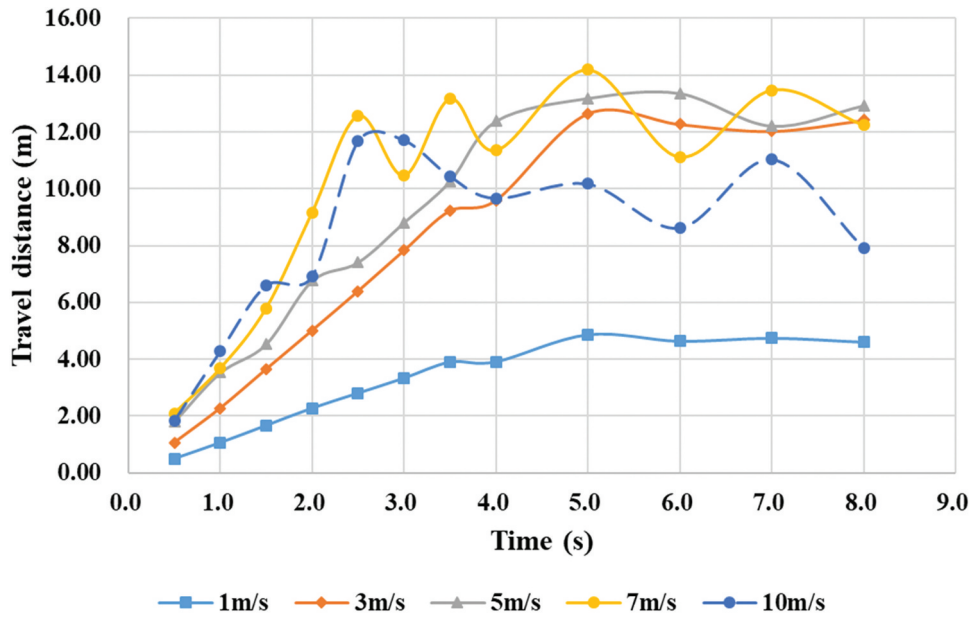| Wind velocity (m/s)	Maximum horizontal distance (m)	Maximum vertical distance (m)	Mean distance at steady state (m)
1	4.87	2.14	4.05
3	12.65	1.69	6.72
5	13.36	1.21	6.37
7	14.19	1.38	4.64
10	11.71	0.55	4.04

$$\frac{\partial \rho}{\partial t} + \nabla \cdot (\rho \vec{u}) = S_m \tag{1}$$

where;

ρ: density

t: time

υ: velocity

S_m: source term-

Equation (1) is general form of mass conservation equation being able to apply on incompressible and compressible fluids.

The momentum conservation equation

Momentum conservation equation is described as;

$$\frac{\partial}{\partial t}(\rho \vec{u}) + \nabla (\rho \vec{u}\vec{u}) = -\nabla p + \nabla \left(\bar{\bar{\tau}}\right) + \rho \vec{g} + \vec{F} \tag{2}$$

where;

p: static pressure-

$\bar{\bar{\tau}}$: stress tensor

$\rho \vec{g}$: gravitational body force-

$\vec{F}$: external body force-

The stress tensor $\bar{\bar{\tau}}$ is given by;

$$\bar{\bar{\tau}} \mu \left[\left(\nabla \vec{u} + \nabla \vec{u}^T \right) - \frac{2}{3} \nabla \cdot \vec{u} I \right] \tag{3}$$

where;

μ: molecular viscosity

I: unit tensor

other terms: the effect of volume dilation-

Species transport equation

PyroSim can model the dispersion of chemical species by solving conservation equations that mathematically describe convention and diffusion. The solution to the convection-diffusion equation for the ith species predicts the local mass fraction, Y_i, of each species. This conservation equation generally shows a below form.

$$\frac{\partial}{\partial t}(\rho Y_i) + \nabla \cdot (\rho \vec{u} Y_i) = -\nabla \cdot \vec{J_i} + R_i + S_i \tag{4}$$

where;

Y_i: local mass fraction of ith species

$\vec{J_i}$: mass flux of ith species

R_i: net rate of production of species i by chemical reaction-

S_i: rate of creation by addition from the dispersed phase-

The mass flux is calculated as below in turbulent flows;

$$\vec{J_i} = -\left(\rho D_{i,m} + \frac{\mu_t}{Sc_t}\right) \nabla Y_i \tag{5}$$

where;

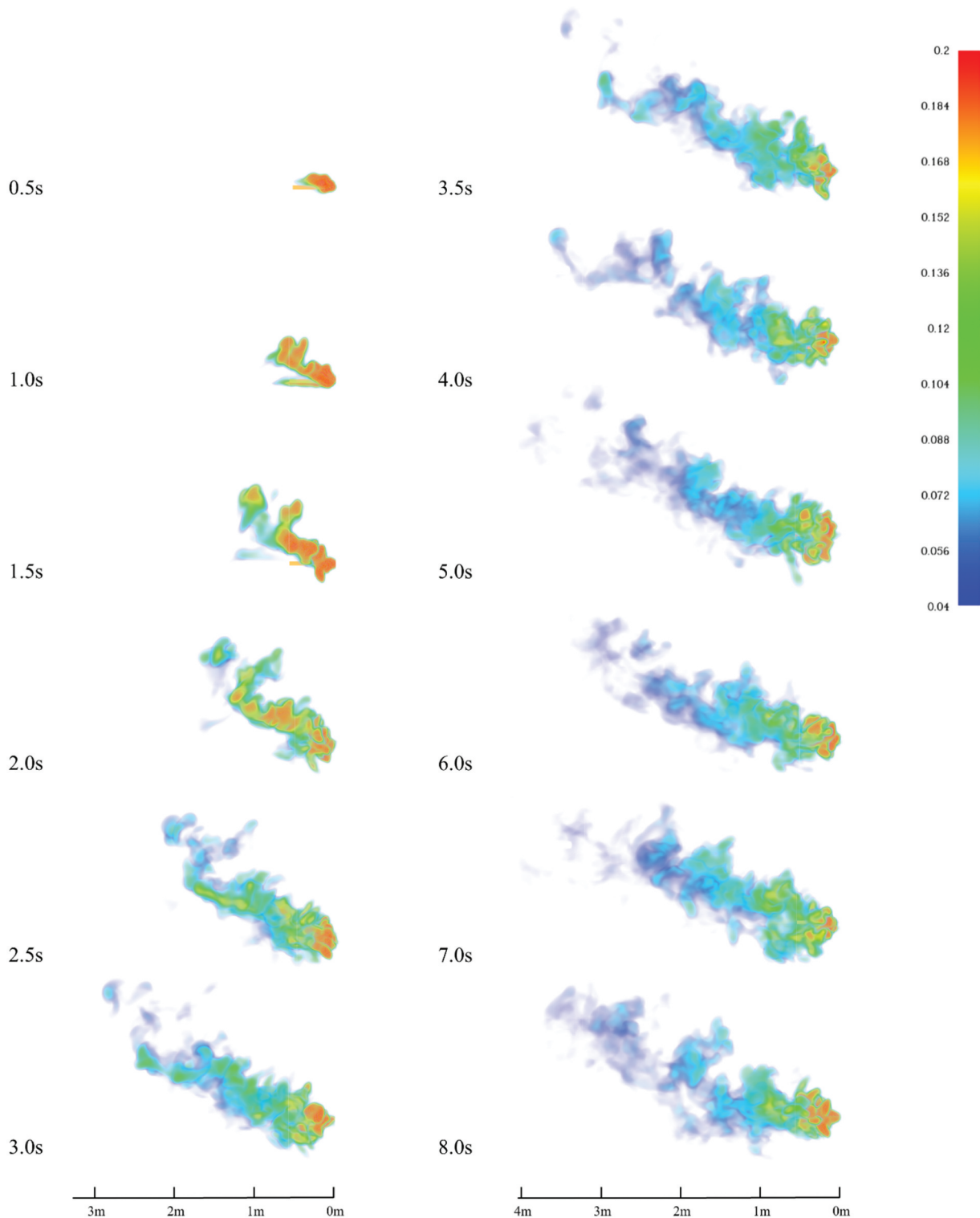$D_{i,m}$: diffusion coefficient for species i in the mixture.

Figure 22. Hydrogen dispersion at 180° and wind velocity 1 m/s (S11).

Hydrogen mass flow

Even though the requirements for the fuel supply rate of hydrogen used in ships have not been specifically determined until now, SAE J261, created by the Society of Automotive Engineers (SAE), describes safe hydrogen supply to vehicles is limited to a maximum fuel supply rate of 1 kg per minute (Van Hoecke et al., 2021). Higher flow rate than that cause adiabatic compression, resulting in excessive heating of the storage system. However, when considering the low energy density of hydrogen and a mass rate of 1 kg/min, the bunkering time required to meet the same energy demand as LNG or ammonia is 86,605 hours per year, and it is unrealistic (DNV, 2021). For this reason, more realistic bunkering duration, a flow rate of 122 m^3/hour is selected according to the same DNV report and this flow rate is calculated based on 3000 kg/hour of mass rate. Even though this flow rate
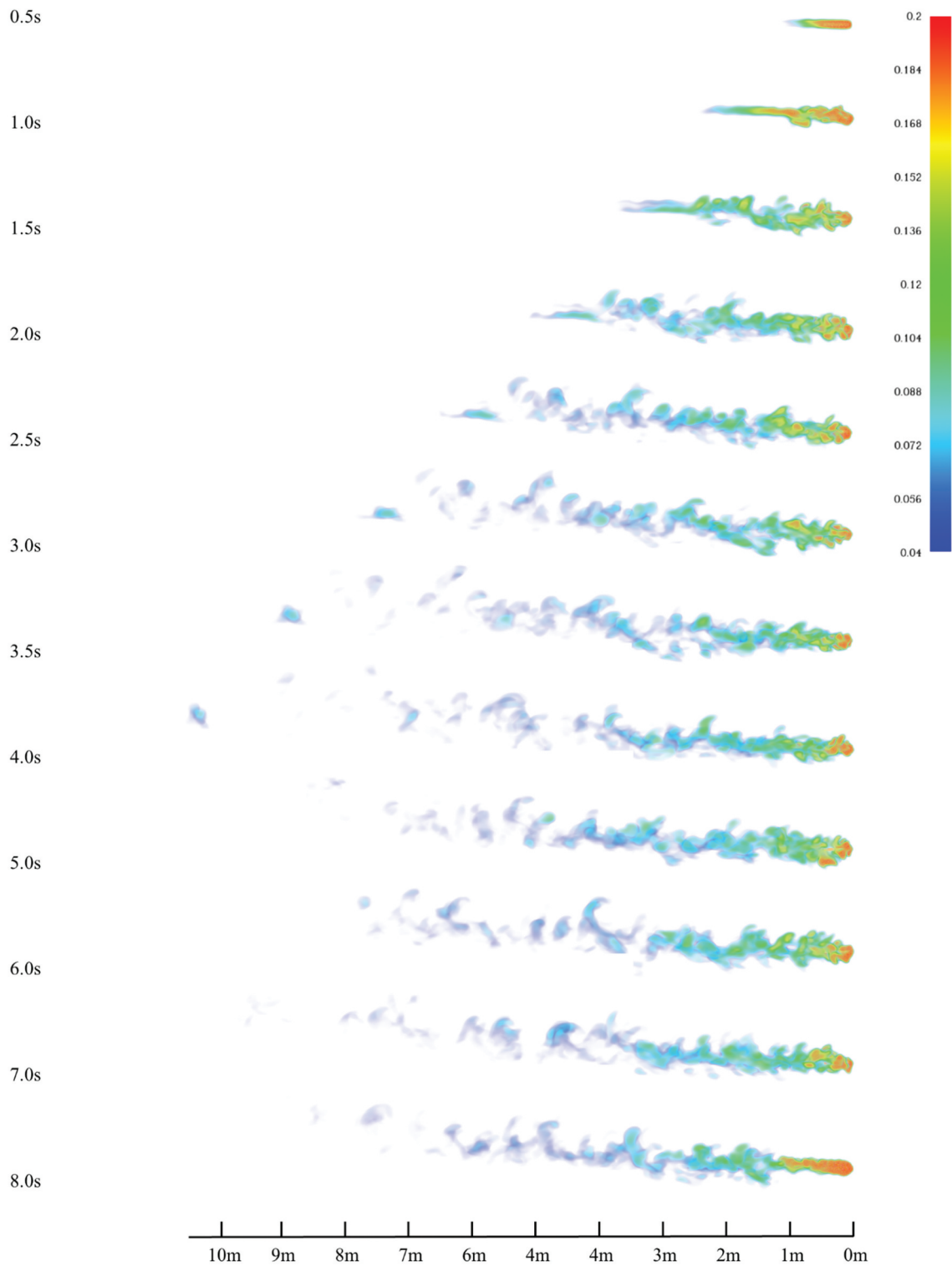
Figure 23. Hydrogen dispersion at 180° and wind velocity 3 m/s (S12).

is claimed that it can be bunkered with any risk in the report, but this is not further proved for a feasibility. Nevertheless, flow rate of 122 m³/hour is much more realistic number. Therefore pressure and flow rate is determined as shown in Table 5. The hose diameter is also determined from the report. Table 5 further indicates volume flow rate and hose diameter at leakage point comparing to the other energy resources.

Definition of leakage scenarios

Hydrogen gas is known for its lightness, making it highly responsive to even slight wind conditions. Therefore, the behaviour of the gas plume can vary significantly in different ports, seasons, and times of the day, due to variations in local wind characteristics. It is crucial to consider the unique environmental conditions of each region when applying the study's
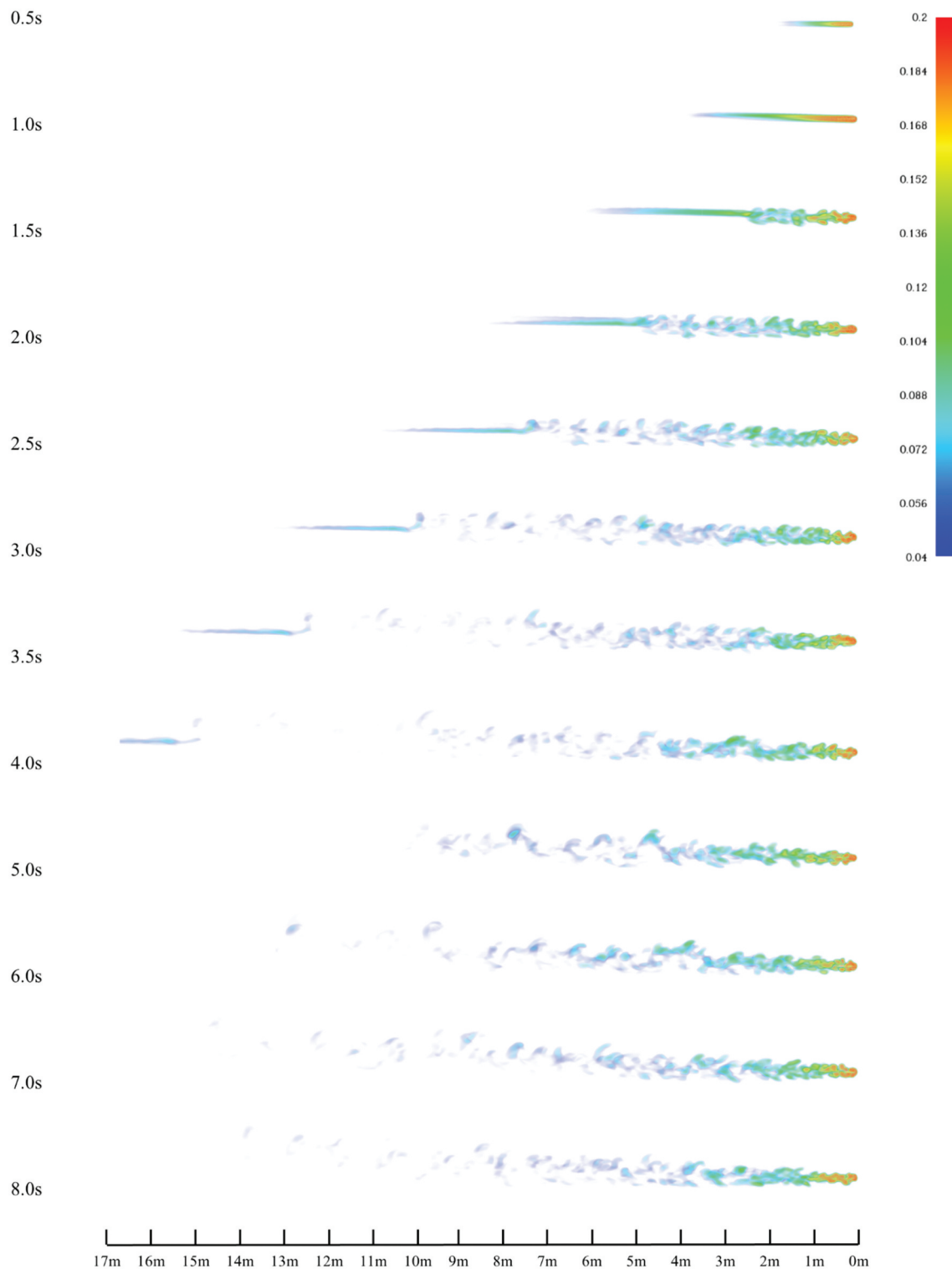
Figure 24. Hydrogen dispersion at 180° and wind velocity 5 m/s (S13).

findings. However, the purpose of this study is not to analyse a specific marine environment in a particular sea area. Instead, the objective is to analyse and compare the behaviour of hydrogen at the leakage point under the influence of typical wind conditions. For this purpose, the wind direction and speed for each scenario were determined. Figure 6 shows wind directions in view of ship location and all scenarios for this study are listed in table 6.

Mesh development

In the case of CFD, the simulation of gas leakage is conducted within a computational mesh. Therefore, the mesh size must provide sufficient space for the gas to diffuse effectively. It is worth noting that smaller cell sizes in the grid result in more accurate solutions. However, on the other hand, a refined grid increases an analysis time. Hence, it is crucial to determine an
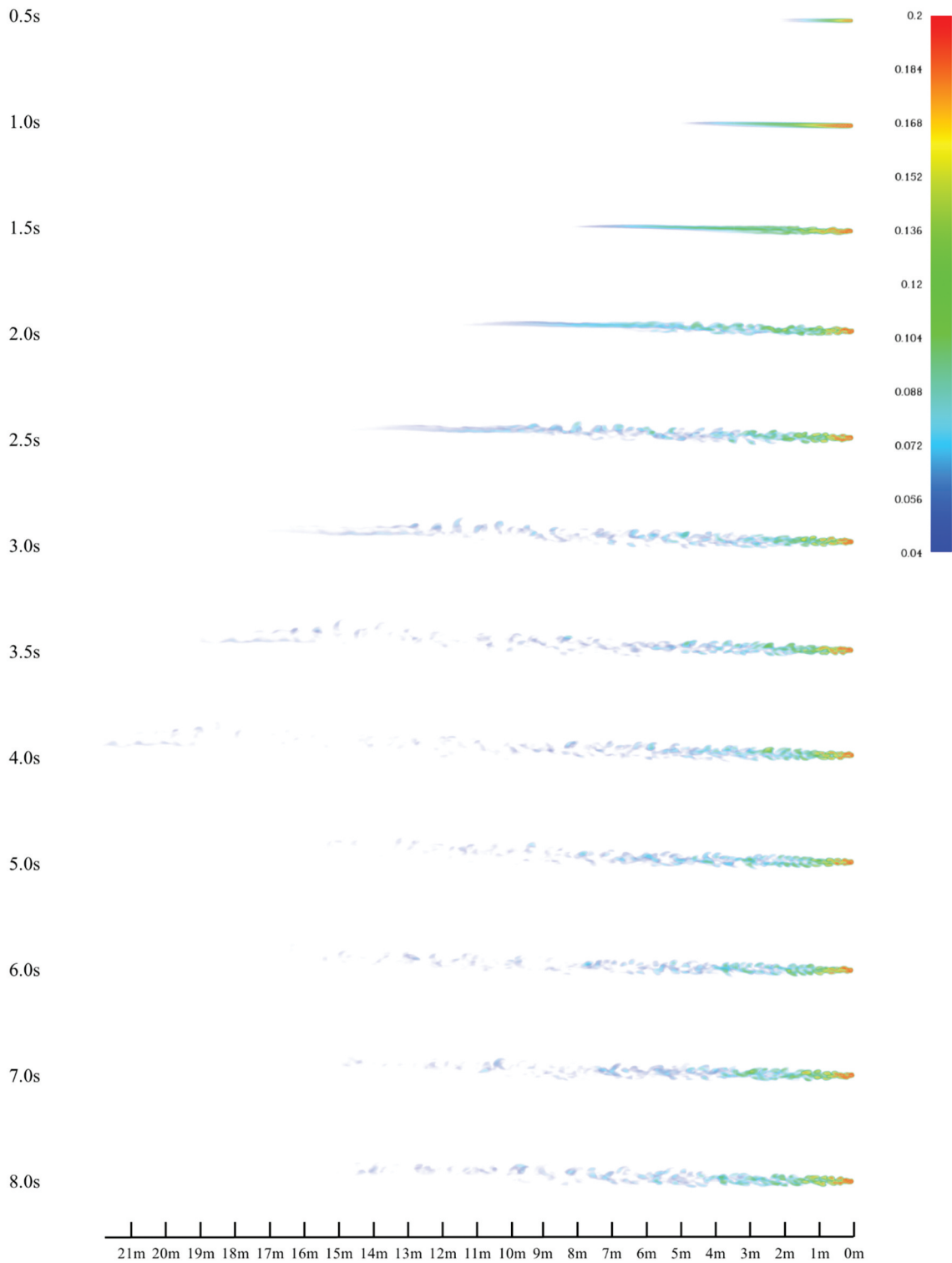
Figure 25. Hydrogen dispersion at 180° and wind velocity 7 m/s (S14).

appropriate number and size of cells. The case studies are performed to determine optimised mesh envelopment and cell size for each scenario. After initially estimating the approximate shape and size of hydrogen leakage for each scenario using a coarse grid, simulations were conducted by applying a finer mesh shape and denser grid.

Figures 7 and Figure 8 show the computational mesh used for the simulation. The mesh size is 25 mm for every scenario, and the number of mesh is various depending on wind direction and velocity. The minimum mesh number is approximately 1.32 million and the maximum is 2.59 million.
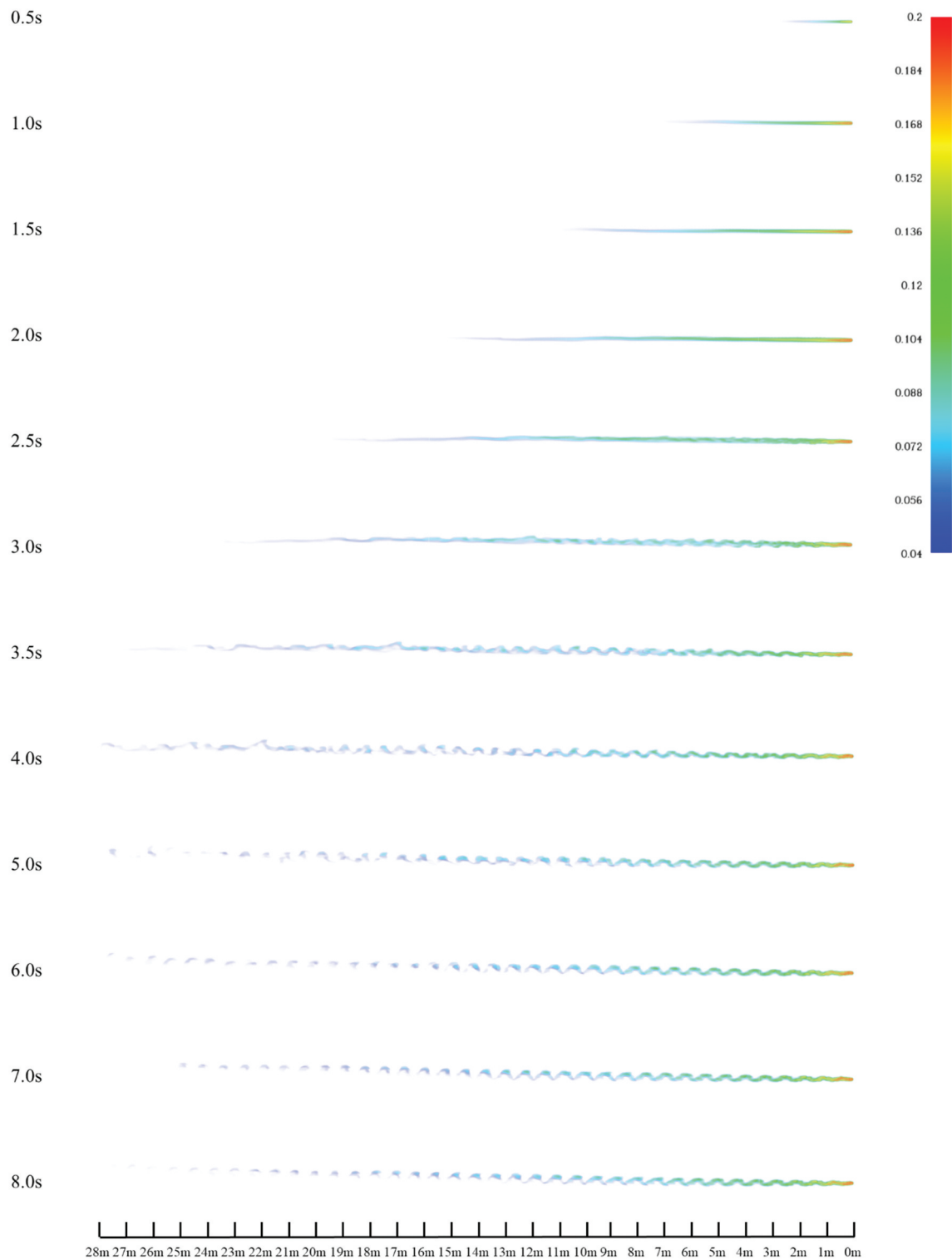
Figure 26. Hydrogen dispersion at 180° and wind velocity 10 m/s (S15).

Boundary conditions

To ensure accurate calculations, it is essential to specify the properties of each boundary surface. Boundary conditions were established based on the default settings in PyroSim, and the definitions of the boundary conditions employed in this simulation are outlined below:

- OPEN: This designation is reserved for vents located on the exterior mesh boundary. An OPEN condition signifies a passive opening to the outside and is commonly utilised to simulate open doors and windows.
- INERT: These surfaces remain at the ambient temperature and do not actively participate in heat
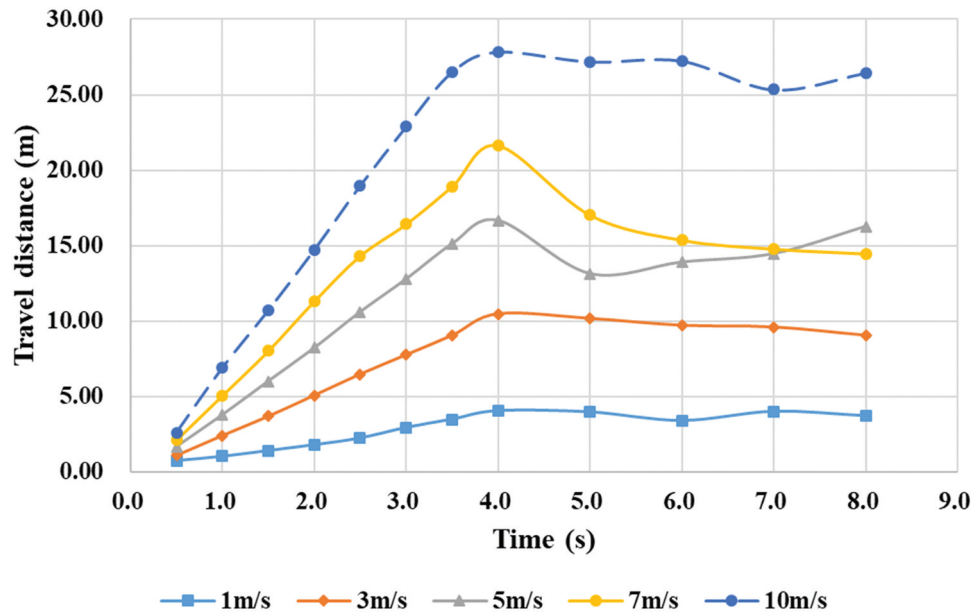
Figure 27. Maximum travel distance of hydrogen at wind direction 180°.

Table 9. Maximum travel distance and steady mean distance for each wind velocity at wind direction 180°.

Wind velocity (m/s)	Maximum horizontal distance (m)	Maximum vertical distance (m)	Mean distance at steady state (m)
1	4.04	2.51	4.00
3	10.46	1.58	5.04
5	16.66	1.40	5.84
7	21.64	1.07	8.12
10	27.85	1.01	14.67

transfer. However, heat transfer can occur from gases to INERT surfaces.

- SUPPLY: This type of surface represents a vent through which gas is injected into the simulation domain.

In this simulation, every boundary surface of the computational mesh was assigned as OPEN to accurately replicate the ship's behaviour while operating at sea. The ship itself can be considered as an obstruction; therefore, the vessel was assigned as INERT. The bunker station is the leakage point, and it was designated as SUPPLY for a continuous gas supply of hydrogen. According to the scenario, the volume flow rate at the leakage point was set to 122 m3/hour according to the simulation scenario. The Figure 9 illustrates the definition of boundary conditions.

Results

The simulation was conducted for an adequate duration following the occurrence of the hydrogen leak at the bunkering station, allowing the hydrogen plume to reach a steady state. This enabled accurate observations and measurements of the

hydrogen's behaviour. The analysis of the simulations primarily focused on the changes in height and length of the hydrogen gas plume under different wind directions and speeds. In this report, only concentrations exceeding 4% volume fraction, which is LFL of hydrogen, were used for analysis. Also, following environmental conditions are applied for all scenarios.

• Ambient temperature	:20.0	°C
• Ambient pressure	:1.01325	bar
• Ambient oxygen mass fraction	:0.232378	kg/kg
• Ambient carbon dioxide mass fraction	:0.000595	kg/kg
• Relative humidity	:40	%
• Specify gravity	:9.81	m/s^2

The Figures (10-14) depict the scenarios, where simulation results from 1 to 5 are captured and listed over time.

The results from each simulation clearly demonstrate a consistent pattern in the behavior of the hydrogen plume throughout the leak period. The height and length of the hydrogen cloud gradually increase in the same direction as the wind. Over time, the plume expands gradually and maintains a constant shape once it reaches a steady state.

The extent of variation in the dimensions of hydrogen dispersion varies with the speed of the airflow. As the wind velocity increases, the length of the gas column tends to grow while the width gradually narrows. This phenomenon is a result of the dynamic interaction between hydrogen and the airflow. With higher wind velocities, a stronger force is exerted on the gas plume, compressing it towards the wind direction and extending its length accordingly.

Another valuable observation is the angle at which the gas plume intersects the horizontal plane. This
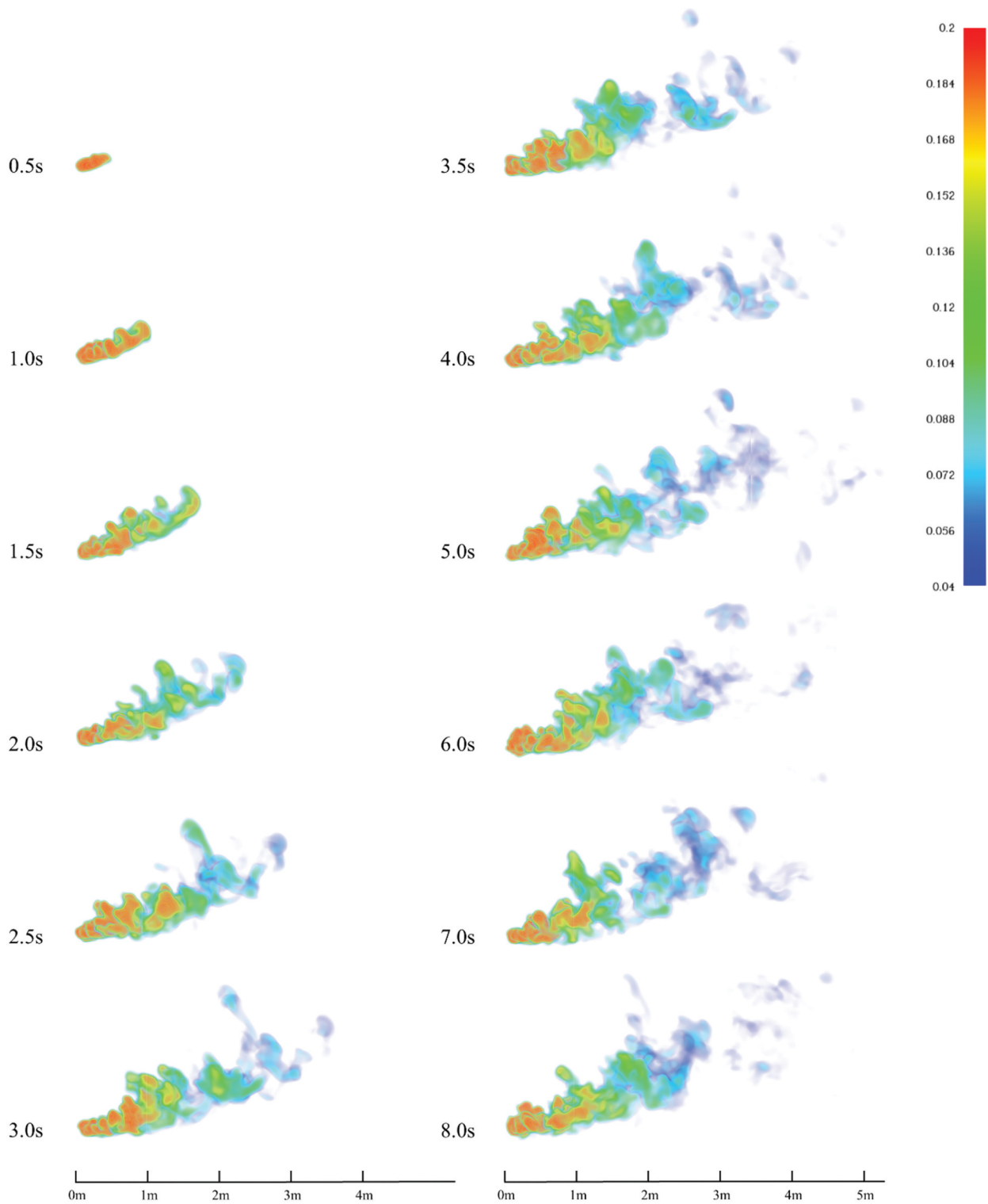
Figure 28. Hydrogen dispersion at 270° and wind velocity 1 m/s (S16)

angle is found to be inversely proportional to the increase in wind velocity. Hydrogen, being lighter than air, initially moves vertically in the absence of wind. However, as the wind velocity increases, the gas column gradually deviates from its vertical trajectory and inclines more towards the horizontal direction. For instance, in the case of S5, where the wind velocity is 10 m/s, it can be observed that the gas column almost aligns with the horizontal surface.

Furthermore, simulations revealed that the formation of hydrogen gas dispersion takes a consistent amount of time to reach a steady state, irrespective of the wind velocity. The steady state signifies the stabilization of gas dispersion and mixing, typically occurring approximately 4 to 5 seconds after the gas leak. Upon reaching the steady state, partial hydrogen groups of a certain size separate from the primary gas plume. However,
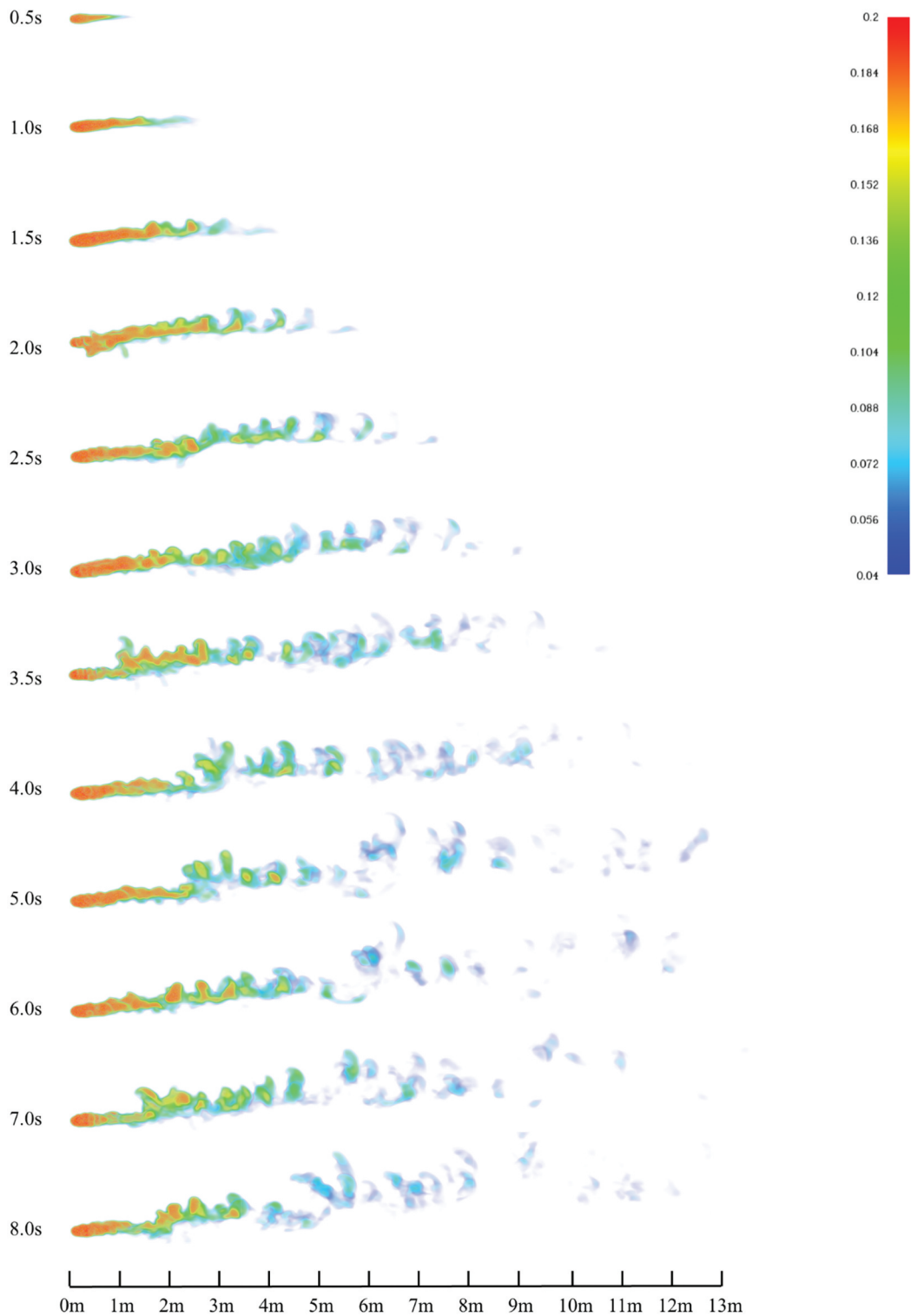
Figure 29. Hydrogen dispersion at 270° and wind velocity 3 m/s (S17).

this is believed to be a result of not expressing the below 4% volume fraction in the analysis.

Following graph shows the maximum travel distance of hydrogen over time at each wind velocity. It indicates that the travelled distance of hydrogen increases proportionally over time until about 4 seconds after the leakage, and when the steady state is reached thereafter, the maximum hydrogen movement distance is consistent. Also, another interesting thing is hydrogen travel distance

is very similar between S4 and S5 even though the shapes, such as the height of the gas plume and the angle with the horizontal plane, are different.

Table 7 presents the average values for the maximum vertical and horizontal distances covered by the gas plume, as well as the mean distance at steady state, for each wind velocity. The mean distance at steady state refers to the average length of the gas plume until the hydrogen leakage reaches a stable condition.
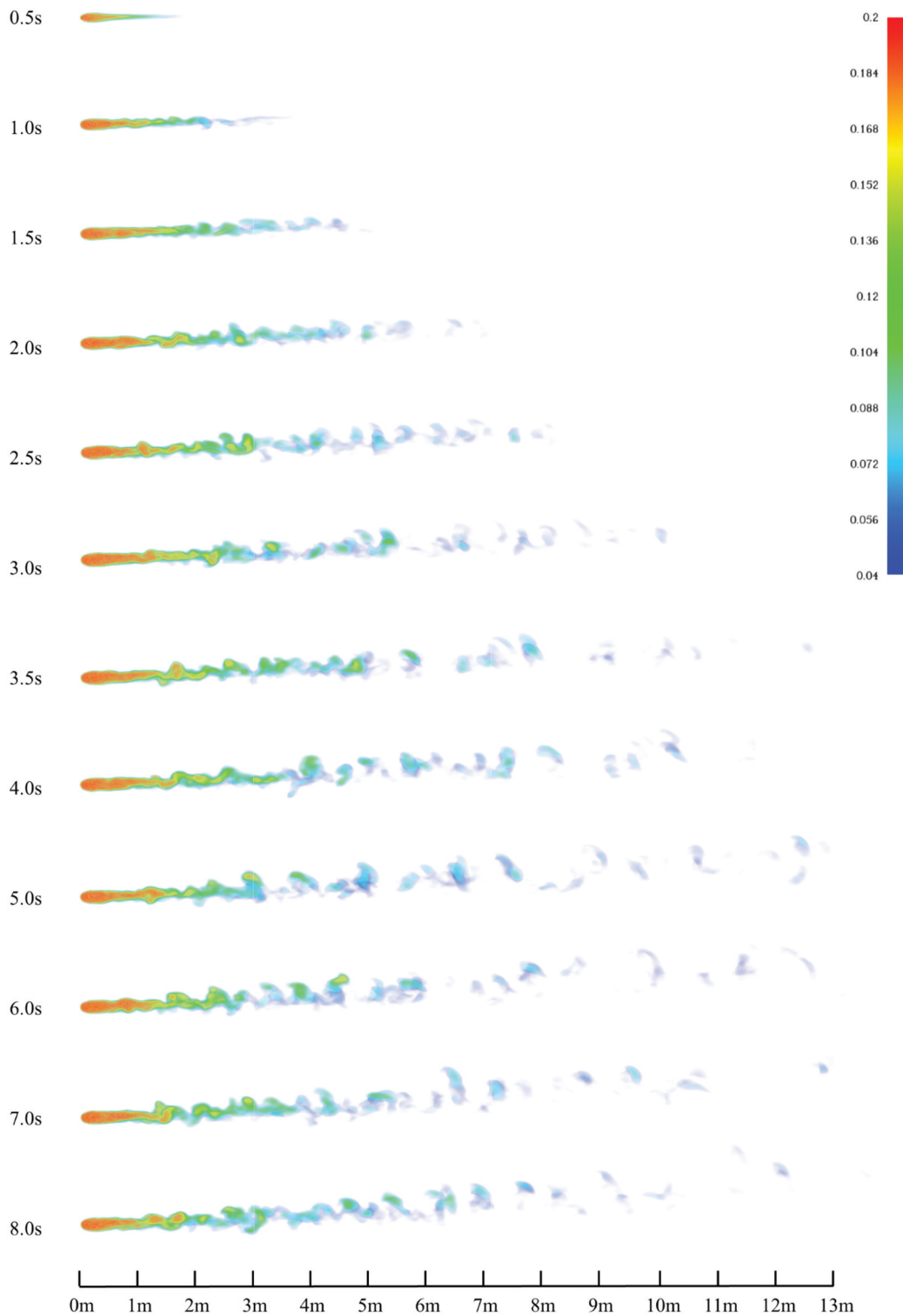
Figure 30. Hydrogen dispersion at 270° and wind velocity 5 m/s (S18).

According to Table 7, it can be observed that the dispersion of the gas plume increases both horizontally and vertically with higher wind velocities, which aligns with the findings from the previous simulation. Furthermore, the mean distance at steady state exhibits the shortest distance in scenario S1, and as the wind velocity gradually increases, the mean distance also proportionally increases, reaching its largest value in scenario S5. Notably, the results for scenarios S4 and

S5 are nearly identical, indicating a similar pattern between the mean distance and the maximum horizontal movement distance. Figure 15 indicates travel distances over the time for wind speed range.

The Figures (16-20) represents the simulation result of scenarios from 6 to 10 which are wind direction of 90°. The results demonstrate a similarity to those obtained at 0° for low wind velocities but show slight differences at high wind velocities.
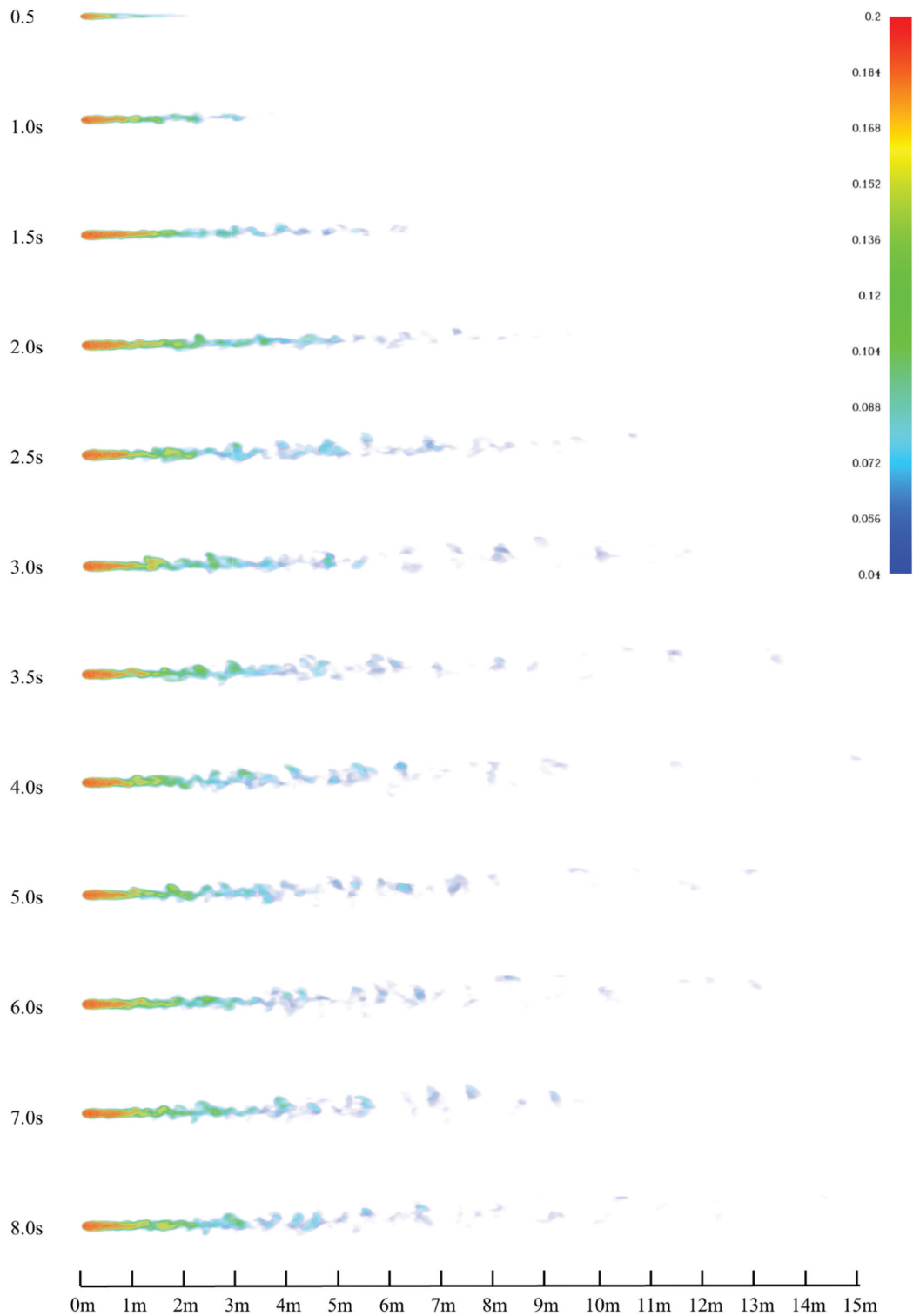
Figure 31. Hydrogen dispersion at 270° and wind velocity 7 m/s (S19).

The fact that the gas plume according to the 90° wind direction analysis coincides with the wind direction and the result of decreasing the angle with the horizontal plane as the wind velocity increases supports the analysis results obtained through the 0° wind direction analysis. This consistent trend shows the effect of wind on the leakage behavior of the gas plume. However, as the wind velocity increases, it clearly shows the difference from the behavior pattern of the gas plume observed under the condition of 0° wind direction.

When analysed for each scenario, the length, width, and angle of the gas plume in S6 are remarkably similar to those of S1. This similarity between the two scenarios can be inferred that at low wind velocities, the gas plume has similar dispersion characteristics regardless of the wind direction. Nevertheless, from S7, as the wind velocity increases, a difference begins to appear from the results observed at 0° wind direction.

In this case, the separation phenomenon in which a separate gas group in the gas plume is separated
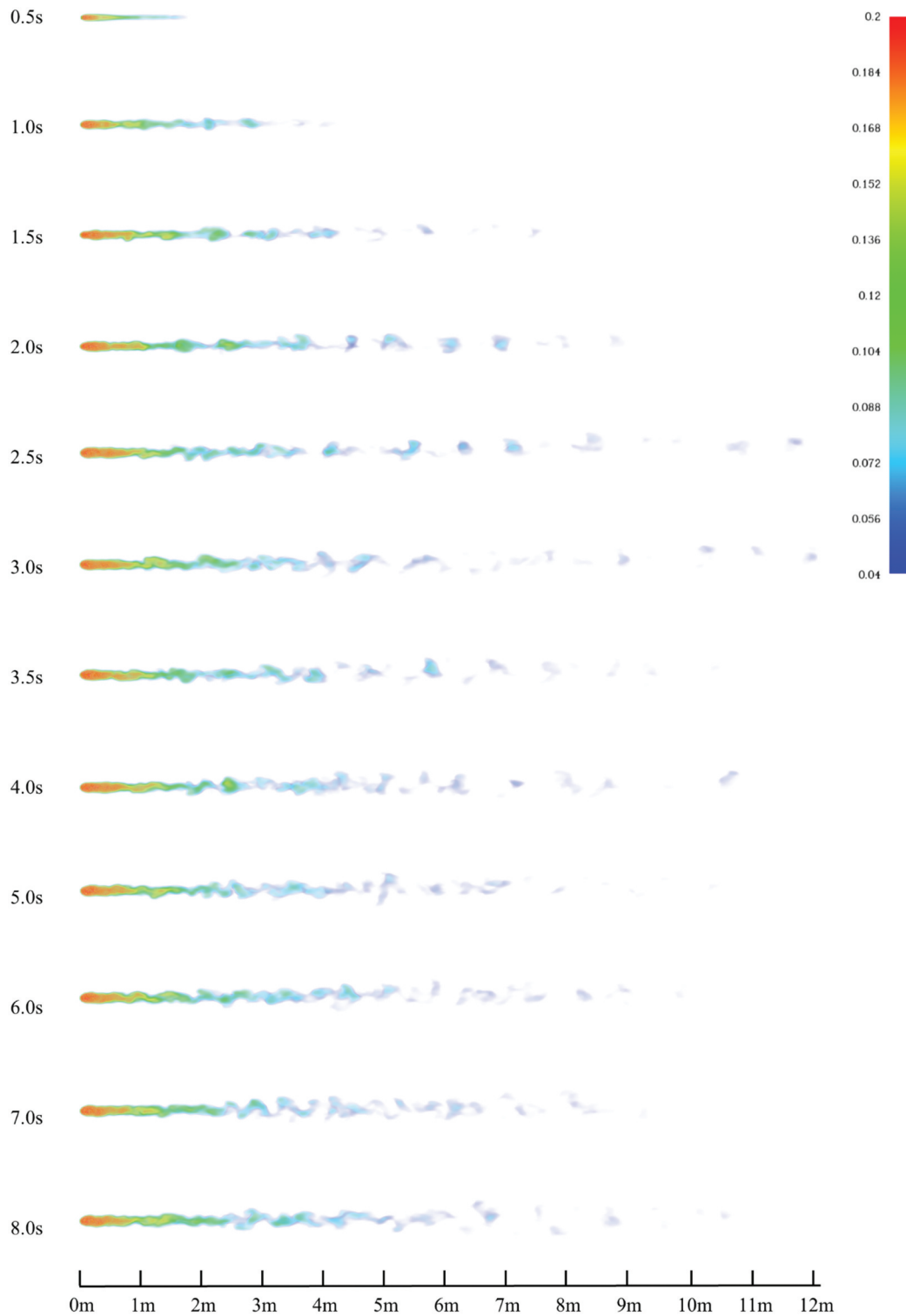
Figure 32. Hydrogen dispersion at 270° and wind velocity 10 m/s (S20).

from the main body occurs relatively quickly within about 1.5 seconds after the hydrogen leak. This phenomenon is considerably faster than the time of about 4 seconds observed in wind direction 0° cases. For other observation points, the differences become more pronounced in subsequent simulations. Separation is accelerated and measurements of the length, width and average distance of the gas plume are significantly smaller than those obtained under the same wind velocity conditions at 0° wind direction. In particular, these differences progressively increase as the wind velocity continues to increase.

The Figure 21 illustrates the maximum horizontal displacement per second for each wind velocity at a wind direction of 90°. As mentioned earlier, at wind velocities of 1 m/s and 3 m/s, the gas plume has a dispersion pattern similar to that observed under a wind direction of 0°. However, at higher wind velocities, the gas plume behaves differently as that the travel distance decreases as wind

Figure 33. Maximum travel distance of hydrogen at wind direction 270°.

Table 10. Maximum travel distance and steady mean distance for each wind velocity at wind direction 270°.

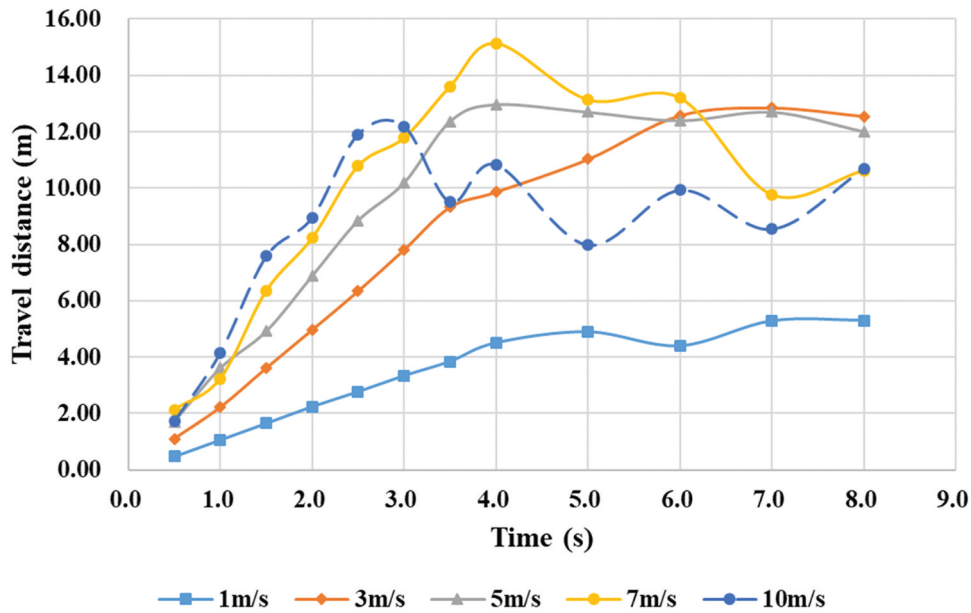| Wind velocity (m/s)	Maximum horizontal distance (m)	Maximum vertical distance (m)	Mean distance at steady state (m)
1	5.30	2.78	3.39
3	12.85	1.96	4.49
5	12.97	1.48	5.75
7	15.14	0.76	5.49
10	12.19	0.58	5.55

velocity increases. The consistency between the mean distance and the horizontal distance is evident from the data presented in the Table 8.

The results shown in Figures (22-26) enable interpretation of the behaviour of the gas plume in scenarios S11 to S16. The analysis result for the wind direction of 180° is found to show a significant difference from the pattern analysed in the previous simulation results performed at wind directions of 0° and 90°.

The most notable feature in the analysis results is that the partial gas plume in the form of a laminar flow, similar to an arrow shot forward, gradually moves in the horizontal direction with the passage of time within the main gas plume. This peculiar phenomenon only occurs in simulations where the wind blows in the opposite direction (180°) from the hydrogen gas leak. The existence of this phenomenon can be confirmed in all simulations of 180° wind direction. This phenomenon gradually becomes evident up to S13 when the wind velocity reaches 5 m/s, and after being seen most clearly at S13, the trace gradually becomes faint as the wind velocity increases. Since the only differences between the wind direction of 0° and 180° are the gas leakage direction and the wind direction, it is clear that this fact is the cause of this phenomenon,

but a more detailed mechanical cause analysis is not covered in this report.

Aside from this notable observation, the main characteristics that can be identified in the gas dispersion are very similar to those obtained for a wind direction of 0°. This suggests that the fundamental properties of gas dispersion remain consistent regardless of wind direction, whereas the unique dynamics associated with a 180° wind direction have distinct behavioural patterns.

The Figure 27 illustrates the maximum horizontal movement at wind direction 180°. In all scenarios, the maximum moving distance was recorded at about 4 seconds, and thereafter, it showed a tendency to decrease. This time coincides with the disappearance of the gas plume of the laminar flow type, the movement distance to reach the peak and the phenomenon of stabilisation after this time, and it is very similar to the analysis results of the 0° wind direction. However, at the fastest wind velocity of 10 m/s, it has a far greater moving distance in the wind direction of 180° than in the wind direction of 0°.

Overall, it is shown in Table 9 that simulation results are very close to the wind direction of 0° except for the maximum horizontal travel distance.

The analysis results for a wind direction of 270° captured in Figures 28-32. The results exhibit similar dispersion patterns to those observed for a wind direction of 90° across all wind velocity categories. Notably, in both cases, the maximum travel distance is not achieved at the highest wind velocity of 10 m/s. Considering that the wind direction is perpendicular to the direction of hydrogen leakage in both scenarios, this phenomenon can be attributed to this particular alignment. However, it is important to note that the
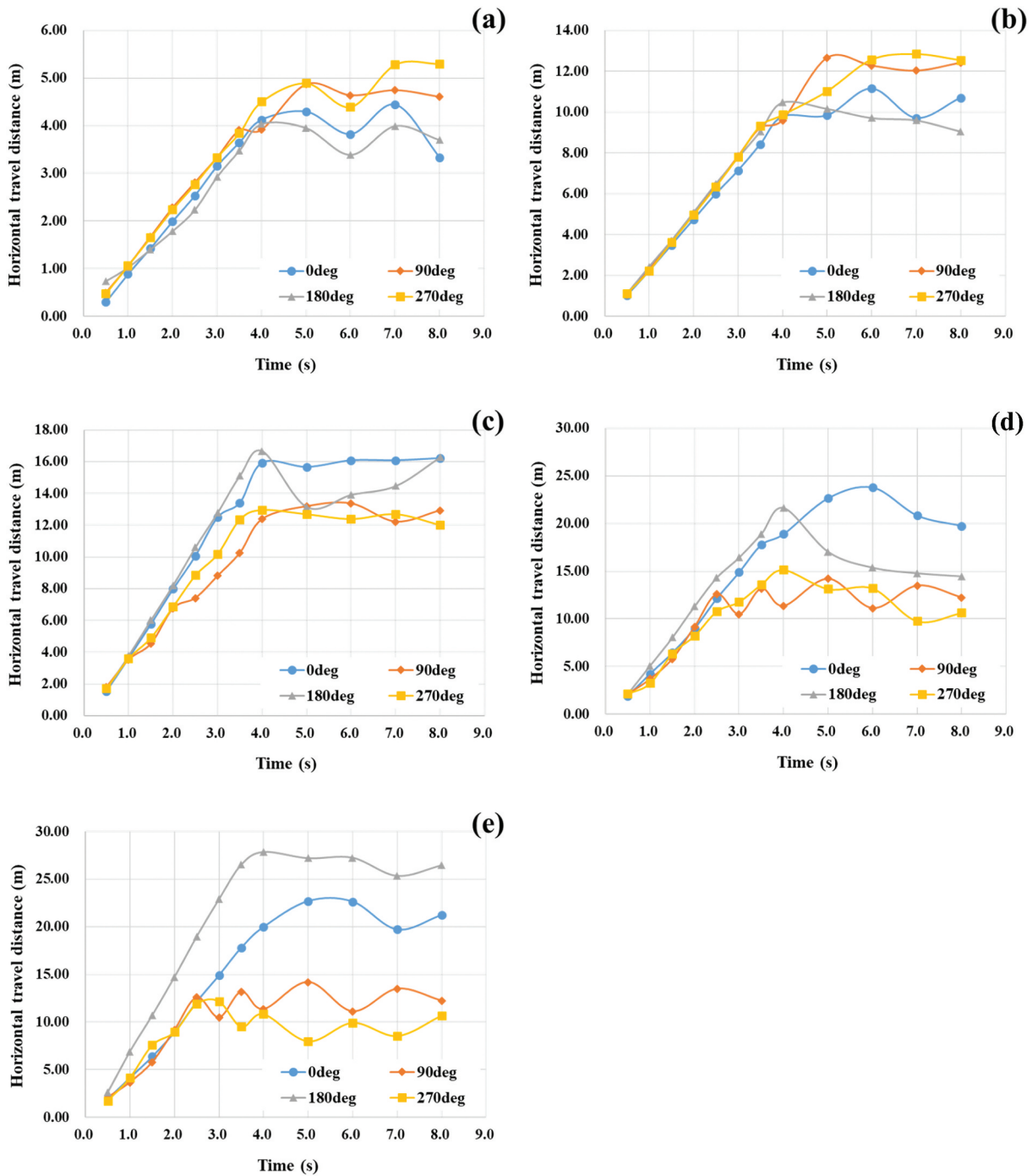
Figure 34. Horizontal travel distance over time (a) wind velocity 1m/s, (b) wind velocity 3m/s, (c) wind velocity 5m/s, (d) wind velocity 7m/s, (e) wind velocity 10m/s.

detailed cause analysis of this phenomenon falls outside the scope of this report, which focuses on physical and epidemiological analysis.

Figure 33 illustrates the measurement of horizontal movement distance over time for each wind velocity in the case of a wind direction of 270°. Across all speed ranges, the maximum horizontal movement distance occurs approximately 3 to 4 seconds after the leak initiation, and this observation is consistent with the data presented in Table 10. The mean distances reported in Table 10 demonstrate similar trends at wind velocities of 5 m/s, 7 m/s, and 10 m/s.

Figure 34 presents graphs that compare the horizontal movement distances over time for different wind directions. Observing each figure, it provides an evidence that the horizontal travel distance remains relatively consistent across all wind direction segments up to a certain point in time. This consistency persists for approximately 4 seconds after the occurrence of a leakage for wind velocities ranging from 1 to 5 m/s and around 3 seconds for wind velocities exceeding this range. Another notable characteristic is observed in the low wind velocity range, where the horizontal dispersion distance is longer when the wind direction

is perpendicular to the direction of hydrogen leakage (90° and 270°) compared to the scenario where the hydrogen leak aligns in a straight line (0° and 180°). However, as the wind velocity increases, the difference gradually becomes more pronounced. Interestingly, after reaching a critical point, the phenomenon reverses, resulting in a contrasting pattern. This phenomenon can be attributed to the persistence of a partial laminar flow gas within the gas plume immediately after the leak, which maintains its shape and propels the dispersion. Contrary to the initial prediction that the maximum movement distance would align with the wind direction corresponding to the leak direction, the simulation results revealed a different outcome. The scenario S15 (180°, 10 m/s) demonstrated the greatest movement distance, reaching a maximum distance of 27.85 meters approximately 4 seconds after the leak initiation. The observed phenomenon can be attributed to the influence of the aforementioned laminar flow movement.

The maximum mean distance after steady state for each direction is summarised in Figure 35.

Across the range of wind speeds considered in the simulation, the average distance after steady condition of the gas plume exhibits consistent changes for each wind direction within the low wind speed range of 1 m/s to 5 m/s. However, a distinct pattern emerges in the high wind speed range. When the leakage direction and wind direction are perpendicular, the mean distance decreases as the wind speed increases. On the other hand, when the leakage direction and wind direction align horizontally, the average distance increases at a much faster rate compared to the low-speed range. At a wind speed of 10 m/s, the difference in average distance between these two cases is approximately threefold.

Discussion

The objective of this study is to use CFD to predict the behaviour of the gas plume under different wind speeds and directions, specifically in the context of small-scale hydrogen-fuelled ships. However, it is important to acknowledge the limitations of this study when applying the findings to specific situations. These limitations can be summarised as follows:

(a) Limitation of wind direction

The main deck of the ship has air vent openings, doors, louver vents, etc., through which leaked hydrogen gas can flow into closed safe areas. Without sufficient ventilation in this space, there is a risk of fire or explosion due to continuous hydrogen inflow. Therefore, analysing the potential interference with the ship's structure and gas behaviour in case of leakage becomes a critical design consideration. This paper examines the shape of the hydrogen plume in four directions: 0°, 90°, 180°, and 270° from the ship. However, in all cases, there was no unintentional interference with the ship's structure or outfitting, making it difficult to confirm the ship's shape effect on hydrogen dispersion.

(b) Potential impacts of hydrogen leakage:

In cases where the direction of gas leakage aligns with the wind direction, there is a risk that hydrogen gas may affect port facilities or other ships supplying hydrogen, depending on the distance from the target ship. The potential effects on the surrounding environment need to be carefully considered and mitigated.
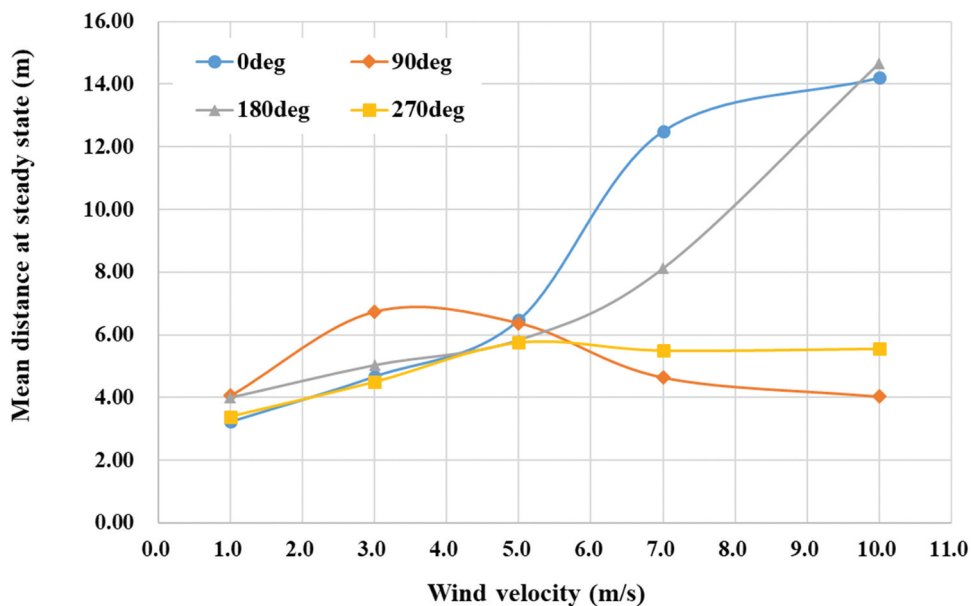

Figure 35. The maximum mean distance at steady state over time for different wind directions.

Despite such limitations, this study provides valuable insights into understanding the behaviour of hydrogen gas plumes under different wind directions and velocities, particularly in unobstructed conditions. This information serves as essential criteria at early development stage for designing ship bunker stations and helps establish the risk boundaries associated with hydrogen leakage based on specific wind environments around the bunker station. However, for broader applicability of this report, it is important to consider scenarios beyond specific wind directions and speeds, such as situations where the wind is vertical or in the opposite direction. In these cases, the movement distance of hydrogen may be shortened or affected by additional physical, epidemiological, and chemical factors. Therefore, further analysis is required to investigate these causes and their implications.

Conclusion

Hydrogen is undoubtedly the most promising energy source for achieving net-zero emissions, not only in the shipping sector but across all industries. However, it is crucial to acknowledge that hydrogen presents unique challenges in terms of its flammability, with a wide range of flammable volume fractions and a high risk of fire due to its low ignition energy. Furthermore, hydrogen fires are difficult to detect due to their low radiant heat and absence of smoke generation. Therefore, to utilise hydrogen as a fuel for ships, it is imperative to understand its characteristics and implement necessary safety measures to prevent fires and accidents, as well as develop mitigation strategies to minimize damage in the event of hydrogen leakage. This report aims to provide insights into the general behaviour of gas dispersion during hydrogen leakage incidents and establish criteria for early-stage design by presenting precautionary measures and safety protocols.

The subsequent sections of this report provide an explanation of the results obtained through CFD simulations for each wind direction.

(a) Wind direction 0°

In all wind speed ranges, the horizontal movement distance of the gas plume increases proportionally with time for approximately 4 seconds after the occurrence of the gas leak. After this period, the gas plume reaches a steady state, and the horizontal movement distance remains relatively constant. The movement distance tends to increase as the wind speed rises from 1 m/s to 5 m/s, but there is little difference in the movement distance between 7 m/s and 10 m/s. The mean distance, however, steadily increases across all speed ranges. The maximum horizontal movement distance and mean distance recorded were 22.68 m and 14.21 m, respectively, at a wind speed of 10 m/s.

(b) Wind direction 90°

The separation of a partial gas plume occurs within approximately 1.5 seconds, which is significantly faster than the 4 seconds observed for a wind direction of 0°. The maximum horizontal movement distance tends to increase with higher wind speeds, similar to the 0° wind direction, but the rate of increase diminishes noticeably after a wind speed of 5 m/s and even decreases at a wind speed of 10 m/s. As for the mean distance, this reversal phenomenon occurs at a faster rate, and at 10 m/s, the smallest value is recorded across the entire speed range. The maximum vertical movement distance observed was 14.19 m at a wind speed of 7 m/s, and the mean distance was 6.72 m at a wind speed of 3 m/s.

(c) Wind direction 180°

The most distinct phenomenon observed at a wind direction of 180 degrees is the maintenance of a laminar flow gas plume, which retains its shape and moves forward over time without transitioning to turbulent flow. This phenomenon is most pronounced at a wind speed of 5 m/s. As a result, the longest horizontal movement distance is observed approximately 4 seconds after the leak. Other characteristics across various wind speeds are quite similar to those observed at a wind direction of 0°. The maximum horizontal movement distance and mean distance recorded in this case were 27.84 m and 14.67 m, respectively, both occurring at a wind speed of 10 m/s.

(d) Wind direction 270°

The dispersion behaviour of hydrogen closely resembles that observed at a wind direction of 90°. Up to approximately 3 seconds after the leak, the moving distance increases with higher wind speeds, but after that point, an inverse relationship emerges where the moving distance tends to decrease as wind speed increases. Consequently, after 7 seconds, the moving distance increases in inverse proportion to speed in all speed ranges except for a wind speed of 1 m/s. The maximum horizontal movement distance recorded in this case was 15.14 m at a wind speed of 7 m/s, and the maximum mean distance was 5.75 m at a wind speed of 5 m/s.

A common feature observed in all wind direction cases is that the hydrogen plume moves in the same direction as the wind, with the length of the plume tending to increase while the width narrows until it stabilises after a certain period of time. Once it reaches a stable state, the plume maintains a consistent shape.

Furthermore, within the speed range of 1 to 5 m/s, the horizontal movement distance exhibits similar characteristics across all wind directions for approximately 4 seconds after the leak and for approximately 3 seconds at wind speeds of 7 m/s and 10 m/s.

The difference between the wind direction and the direction of hydrogen leakage also significantly impacts the dispersion behaviour of hydrogen. When the directions are perpendicular, the travel distance generally increases gradually with higher wind speeds, whereas in the case of opposite directions, the gas plume's distance tends to decrease at high speeds. Interestingly, the largest movement distance of 27.85 m was observed at a wind direction of 180°, where the leak direction and wind direction are in opposite directions. This phenomenon can be attributed to the previously mentioned laminar gas plume.

Regarding the mean distance, a similar increase is evident in all wind directions up to a wind speed of 5 m/s or less. However, starting from a wind speed of 7 m/s, the scenarios where the wind direction is horizontal or vertical exhibit distinct differences. In the horizontal cases, the mean distance shows a rapid increase, reaching approximately three times the value observed in the vertical cases at a wind speed of 10 m/s.

Disclosure statement

No potential conflict of interest was reported by the author(s).

ORCID

Byongug Jeong ⓘ http://orcid.org/0000-0002-8509-5824

References

ABS, GUIDE FOR LNG BUNKERING, in: A.A.B.o. Shipping (Ed.). 2016

Ahn, S. I., Kurt, R. E., & Turan, O. (2022). The hybrid method combined STPA and SLIM to assess the reliability of the human interaction system to the emergency shutdown system of LNG ship-to-ship bunkering. *Ocean Engineering*, *265*, 112643. https://doi.org/10.1016/j.oceaneng.2022.112643

Atilhan, S., Park, S., El-Halwagi, M. M., Atilhan, M., Moore, M., & Nielsen, R. B. (2021). Green hydrogen as an alternative fuel for the shipping industry. *Current Opinion in Chemical Engineering*, *31*, 100668. https://doi.org/10.1016/j.coche.2020.100668

Blaylock, M., & Klebanoff, L. (2022). Hydrogen gas dispersion studies for hydrogen fuel cell vessels I: Vent mast releases. *International Journal of Hydrogen Energy*, *47*(50), 21506–21516. https://doi.org/10.1016/j.ijhydene.2022.04.262

Bouman, E. A., Lindstad, E., Rialland, A. I., & Strømman, A. H. (2017). State-of-the-art technologies, measures, and potential for reducing GHG emissions from shipping–A review, transportation research part D. *Transport and Environment*, *52*, 408–421. https://doi.org/10.1016/j.trd.2017.03.022

Brzezińska, D. (2021). Hydrogen dispersion phenomenon in nominally closed spaces. *International Journal of Hydrogen Energy*, *46*(55), 28358–28365. https://doi.org/10.1016/j.ijhydene.2021.06.061

Choi, J., Hur, N., Kang, S., Lee, E. D., & Lee, K.-B. (2013). A CFD simulation of hydrogen dispersion for the hydrogen leakage from a fuel cell vehicle in an underground parking garage. *International Journal of Hydrogen Energy*, *38*(19), 8084–8091. https://doi.org/10.1016/j.ijhydene.2013.02.018

C. IMO. (2020). *Fourth IMO GHG study 2020*. International Maritime Organization (IMO).

Dadashzadeh, M., Ahmad, A., & Khan, F. (2016). Dispersion modelling and analysis of hydrogen fuel gas released in an enclosed area: A CFD-based approach. *Fuel*, *184*, 192–201. https://doi.org/10.1016/j.fuel.2016.07.008

De Stefano, M., Rocourt, X., Sochet, I., & Daudey, N. (2019). Hydrogen dispersion in a closed environment. *International Journal of Hydrogen Energy*, *44*(17), 9031–9040. https://doi.org/10.1016/j.ijhydene.2018.06.099

DNV. (2021). *External safety study - bunkering of alternative marine fuel for seagoing vessels*. Amsterdam: DNV B.V.

Durbin, D., & Malardier-Jugroot, C. (2013). Review of hydrogen storage techniques for on board vehicle applications. *International Journal of Hydrogen Energy*, *38*(34), 14595–14617. https://doi.org/10.1016/j.ijhydene.2013.07.058

Goswami, R., & Sun, B. (2022). Study on vapour dispersion and explosion from compressed hydrogen spill: Risk assessment on a hydrogen plant. *International Journal of Hydrogen Energy*, *47*(97), 41195–41207. https://doi.org/10.1016/j.ijhydene.2022.09.190

G.S. CENTER. (2021). Sustainability whitepaper hydrogen as marine fuel, in, ABS (American Bureau of Shipping).

He, J., Kokgil, E., Wang, L. (., & Ng, H. D. (2016). Assessment of similarity relations using helium for prediction of hydrogen dispersion and safety in an enclosure. *International Journal of Hydrogen Energy*, *41*(34), 15388–15398. https://doi.org/10.1016/j.ijhydene.2016.07.033

Huang, T., Zhao, M., Ba, Q., Christopher, D. M., & Li, X. (2022). Modeling of hydrogen dispersion from hydrogen fuel cell vehicles in an underground parking garage. *International Journal of Hydrogen Energy*, *47*(1), 686–696. https://doi.org/10.1016/j.ijhydene.2021.08.196

Hyde, K., Ellis, A., & Power, I. (2019). *Feasibility of hydrogen bunkering*. ITM Power.

Hysafe. (2007). Hydrogen Fundamentals. Accessed June 2, 2023, from http://www.hysafe.org/download/1196/BRHS_Chap1_V1p2.pdf

IMO. (2018). *Adoption of the initial IMO strategy on reduction of GHG emissions from ships and existing IMO activity related to reducing GHG emissions in the shipping sector*. London: IMO.

Inal, O. B., Zincir, B., & Deniz, C. (2022). Investigation on the decarbonization of shipping: An approach to hydrogen and ammonia. *International Journal of Hydrogen Energy*, *47*(45), 19888–19900. https://doi.org/10.1016/j.ijhydene.2022.01.189

Kim, B., & Hwang, K.-I. (2022). Numerical analysis of the effects of ship motion on hydrogen release and dispersion in an enclosed area. *Applied Sciences*, *12*(3), 1259. https://doi.org/10.3390/app12031259

Kim, B., & Hwang, K.-I. (2023). Experimental analysis of the effects of ship motion on hydrogen dispersion in an

enclosed area. *International Journal of Hydrogen Energy*, *48*(81), 31779–31789. https://doi.org/10.1016/j.ijhydene.2023.04.320

Liu, Y.-L., Zheng, J.-Y., Xu, P., Zhao, Y.-Z., Bie, H.-Y., Chen, H.-G., & Dryver, H. (2009). Numerical simulation on the diffusion of hydrogen due to high pressured storage tanks failure. *Journal of Loss Prevention in the Process Industries*, *22*(3), 265–270. https://doi.org/10.1016/j.jlp.2008.06.007

Middha, P., Hansen, O. R., Grune, J., & Kotchourko, A. (2010). CFD calculations of gas leak dispersion and subsequent gas explosions: Validation against ignited impinging hydrogen jet experiments. *Journal of Hazardous Materials*, *179*(1–3), 84–94. https://doi.org/10.1016/j.jhazmat.2010.02.061

Middha, P., Hansen, O. R., & Storvik, I. E. (2009). Validation of CFD-model for hydrogen dispersion. *Journal of Loss Prevention in the Process Industries*, *22*(6), 1034–1038. https://doi.org/10.1016/j.jlp.2009.07.020

Moradi, R., & Groth, K. M. (2019). Hydrogen storage and delivery: Review of the state of the art technologies and risk and reliability analysis. *International Journal of Hydrogen Energy*, *44*(23), 12254–12269. https://doi.org/10.1016/j.ijhydene.2019.03.041

Mousavi, J., & Parvini, M. (2016). A sensitivity analysis of parameters affecting the hydrogen release and dispersion using ANOVA method. *International Journal of Hydrogen Energy*, *41*(9), 5188–5201. https://doi.org/10.1016/j.ijhydene.2016.01.042

Qian, J.-Y., Li, X.-J., Gao, Z.-X., & Jin, Z.-J. (2020). A numerical study of hydrogen leakage and diffusion in a hydrogen refueling station. *International Journal of Hydrogen Energy*, *45*(28), 14428–14439. https://doi.org/10.1016/j.ijhydene.2020.03.140

Ratnakar, R. R., Gupta, N., Zhang, K., van Doorne, C., Fesmire, J., Dindoruk, B., & Balakotaiah, V. (2021). Hydrogen supply chain and challenges in large-scale LH2 storage and transportation. *International Journal of Hydrogen Energy*, *46*(47), 24149–24168. https://doi.org/10.1016/j.ijhydene.2021.05.025

Shu, Z., Liang, W., Zheng, X., Lei, G., Cao, P., Dai, W., & Qian, H. (2021). Dispersion characteristics of hydrogen leakage: Comparing the prediction model with the experiment. *Energy*, *236*, 121420. https://doi.org/10.1016/j.energy.2021.121420

Swain, M., Filoso, P., & Swain, M. (2007). An experimental investigation into the ignition of leaking hydrogen. *International Journal of Hydrogen Energy*, *32*(2), 287–295. https://doi.org/10.1016/j.ijhydene.2006.06.041

Tofalos, C., Jeong, B., & Jang, H. (2020). Safety comparison analysis between LNG/LH2 for bunkering operation. *Journal of International Maritime Safety, Environmental Affairs, and Shipping*, *4*(4), 135–150. https://doi.org/10.1080/25725084.2020.1840859

Tretsiakova McNally, S., Hydrogen fires, in, Hyresponse.

Van Hoecke, L., Laffineur, L., Campe, R., Perreault, P., Verbruggen, S. W., & Lenaerts, S. (2021). Challenges in the use of hydrogen for maritime applications. *Energy & Environmental Science*, *14*(2), 815–843. https://doi.org/10.1039/D0EE01545H

Venetsanos, A., Baraldi, D., Adams, P., Heggem, P., & Wilkening, H. (2008). CFD modelling of hydrogen release, dispersion and combustion for automotive scenarios. *Journal of Loss Prevention in the Process Industries*, *21*(2), 162–184. https://doi.org/10.1016/j.jlp.2007.06.016

Ventikos, N., Podimatas, V., & Koimtzoglou, A. (2022). LNG bunkering QRA: A case study on the port of Piraeus. *Journal of Risk Analysis and Crisis Response*, *12*(1). https://doi.org/10.54560/jracr.v12i1.318

Wang, Z., Wang, Y., Afshan, S., & Hjalmarsson, J. (2021). A review of metallic tanks for H2 storage with a view to application in future green shipping. *International Journal of Hydrogen Energy*, *46*(9), 6151–6179. https://doi.org/10.1016/j.ijhydene.2020.11.168

Witcofski, R. D., & Chirivella, J. (1984). Experimental and analytical analyses of the mechanisms governing the dispersion of flammable clouds formed by liquid hydrogen spills. *International Journal of Hydrogen Energy*, *9*(5), 425–435. https://doi.org/10.1016/0360-3199(84)90064-8

Xin, J., Duan, Q., Jin, K., & Sun, J. (2023). A reduced-scale experimental study of dispersion characteristics of hydrogen leakage in an underground parking garage. *International Journal of Hydrogen Energy*, *48*(44), 16936–16948. https://doi.org/10.1016/j.ijhydene.2023.01.170